A Major Project Report

on

TRIBOLOGICAL STUDY OF HYDRODYNAMIC JOURNAL BEARING AND ITS ANALYSIS

Submitted for the partial fulfillment of the requirement for the degree of

Master of Technology

in

Computational Design

Submitted by

Prem Kumar Agarwal (2K15/CDN/11)

under the supervision of

Dr. R. C. Singh — Associate Professor

Sh. Roop Lal — Assistant Professor

Department of Mechanical Engineering

Delhi Technological University

July-2017

DECLARATION

I hereby declare that the thesis entitled **"TRIBOLOGICAL STUDY OF HYDRODYNAMIC JOURNAL BEARING AND ITS ANALYSIS"** which is being submitted to the Delhi Technological University in partial fulfillment of the requirement for the award of the degree of **Master of Technology** in **Computational Design** is an authentic work carried out by me.

Prem Kumar Agarwal

2K15/CDN/11

CERTIFICATE

This is to certify that the dissertation entitled **Tribological Study of Hydrodynamic Journal Bearing and Its Analysis** produced by **PREM KUMAR AGARWAL (M-TECH) (2K15/CDN/11)** in the partial fulfillment of the requirements for the reward of the degree of Master of Technology, Delhi Technological University (Formerly Delhi College of Engineering), is an authentic record of the candidate's own work carried out by him under our guidance**.** The information and data enclosed in this report are original and has not been submitted elsewhere for honoring of any other degree to the best of our knowledge and belief**.**

Dr. R.C.Singh
(Project Mentor)
Associate Professor

Sh.Roop Lal
(Project Mentor)
Assistant Professor

.ACKNOWLEDGEMENTS

Research is a higher concept**.** It brings to test our patience, vigor, and dedication**.** Every result arrived is a beginning for a higher achievement**.** My project is a small drop in an ocean**.** It needs the help of friends and guidance of experts in the field, to achieve something new**.**

I found my pen incompetent to express my thanks to my supervisor **Dr. R.C.Singh, Associate Professor, and Sh. Roop Lal, Assistant Professor, DTU** under their kind and worthy guidance and supervision. I had the opportunity to carry out this work**.** It was only due to their advice, thoughtful comments, constructive criticism, and continuous vigil over the progress of my work with a personal interest that it has taken this shape**.** They have been a great source of encouragement**.**

To get an opportunity to carry out the project work in the well-equipped, ever developing laboratories in our institution, I would like to pay my deep sense of thankfulness to **Prof. R. S. Mishra, HOD, Department of Mechanical Engineering, DTU.**

I would like to express my sincere gratitude and indebtedness to **Prof. Vikas Rastogi, DTU** for prevailing me to do my laboratory work at Design Centre. I am very thankful to him for allowing me to work in his lab and also for providing me guidance. I am highly thankful to **Dr. A.K.Agarwal, Associate Professor, DTU** as he helped me and motivated me towards my work. His suggestion was very thoughtful and impressive and that has inspired me to complete my project.

I am especially thankful to **Sh. Vipin Sharma, Assistant Professor, MAIT, and Sh. Sumit Chaudhary, Ph.D. Scholar, DTU** as I have completed my project under their worthy guidance and supervision. Their advice and thoughtful comments inspired me and were very helpful to complete my project.

I am very much thankful to my parents for their moral support and encouragement, which was giving me the strength to chase my goal. Without their support and inspiration, I would not able to complete my degree.

I would especially like to acknowledge my gratitude to all my dear friends for their consistent support, valuable suggestions from time to time to make this project worthy**.**

With a silent prayer to the Almighty, I take this opportunity to express my gratitude to all those who have supported me in completing my fourth-semester project work as a part of my degree program**.**

PREM KUMAR AGARWAL
2K15/CDN/11

CONTENTS

LIST OF ABBREVIATIONS

∂ - delta

h - minimum oil film thickness

P - pressure

θ - contact angle

R - radius

L - length

∂Z - wedge action along z-axis

μ – dynamic viscosity

$(\omega_1 - \omega_2)$ - stretching action

∂x - wedge action along x-axis

u_1 - initial fluid velocity

u_2 - final fluid velocity

C – clearance

S – sommerfeld number

N – speed in rpm

LIST OF FIGURES

LIST OF TABLES

ABSTRACT

Journal bearing friction pair system is one of the most general and essential parts used in various mechanical devices. The friction and wear behavior of journal bearing material has been investigated using pin and disc. The friction and wear behavior of the journal bearing material has changed according to the sliding conditions and lubricating oils. The behavior of journal bearing must be analyzed to increase its life and performance and to reduce its wear under hydrodynamic lubrication at different conditions.

The objectives of this research are to provide an analysis of the pressure distribution in the lubricant with different speeds of the journal and at different loads for a journal bearing experimentally as well as computationally.

A computational model has been developed and graphical solutions were obtained for the pressure distribution over the bearing surface. The pressure distribution for lubrication film is obtained using MATLAB software graphically. The pressure distribution along with torque and temperature at the outlet of the journal bearing has been obtained experimentally and it was then compared with the theoretical solutions.

Two process parameters, namely radial load & journal speed are considered as the factors influencing the pressure curve of the journal bearing. Experimentation was carried out on the journal bearing rig TR-660 to measure pressure at a different angular position on the bottom half of journal bearing.

Key Words: Journal bearing, hydrodynamic lubrication, pressure distribution, friction, wear.

`

Chapter 1
INTRODUCTION

Study of mechanics of friction and the relationship between friction and wear back to the sixteenth century, almost immediately after the invention of Newton's law of motion. It was observed by several researchers that the variation of friction depends on interfacial conditions such as normal load, geometry, relative surface motion, sliding velocity, the surface roughness of the rubbing surfaces, type of material, system rigidity, temperature, stick-slip, relative humidity, lubrication, and vibration. Among these factors, normal load and sliding velocity are the two major factors that play a significant role for the variation of friction. In the case of materials with surface films which are either deliberately applied or produced by reaction with the environment, the coefficient of friction may not.

1.1 Brief introduction to tribology

Tribology is the science and technology of interacting surfaces in relative motion (and the practices related thereto), including the subject of friction, wear, and lubrication. Tribology comes from the Greek word, **"tribos**", it meaning is "rubbing" or **"to rub**" And from the suffix, "logy" means "the study of" Therefore, Tribology is the study of rubbing, or "the study of things that rub".

This includes the fields of:

• Friction

• Lubrication

• Wear.

`

1.1.1. FRICTION

Friction is a principal cause of wear and energy dissipation. Considerable savings can be made by improved friction control. It is estimated that one-third of the world's energy resources in present use is needed to overcome friction in one form or another.

When one solid body is slide over another so there is some resistance to the motion which is called friction. Considering friction as a nuisance, attempts are made to eliminate it or to diminish it to as small a value as possible. No doubt a considerable loss of power is caused by friction (e.g. about 20% in motor cars, 9% in airplane piston engine and (1 ½ - 2) % in turbojet engines) but more important aspect is the damage that is done by friction – the wear of some vital parts of machines. This factor limits the design and shortens the effective working life of the machines.

1.1.1.1.Laws of friction:

Basically, friction works on five laws which are as follows:

- When an object is moving, the friction is proportional and perpendicular to the normal force (N).
- Friction is independent of the area of contact so long as there is an area of contact.
- The coefficient of static friction is slightly greater than the coefficient of kinetic friction.
- Within rather large limits, kinetic friction is independent of velocity.
- Friction depends upon the nature of the surfaces in contact.

1.1.2. LUBRICATION

Lubrication is an effective means of controlling wear and reducing friction.It is evident that lubrication is required to minimize sliding friction in complete bearings. An additional function of the lubricant is to act as a protection for the accurately ground and highly-polished surfaces of the balls, rollers, and rings. If free moisture is allowed to contact the

`

bearing elements, corrosion and pitting will follow and the bearing life will be considerably shortened. At the same time, a suitable lubricant should prevent the entry of external contaminating matter in the form of dirt or abrasive dust.

1.1.3. WEAR

Wear is the major cause of material wastage and loss of mechanical performance and any reduction in wear can result in considerable savings.

Wear is the actual removal of surface material due to the frictional force between two mating surfaces. This can result in a change in component dimension which can lead to looseness and subsequent improper operation. Wear increases the clearance between the shaft and bearing and leads to a reduction in load support capacity of the bearing. Often such failures occur in absence of sufficient lubricant hydrodynamic film thickness due to relatively low speed. The adhesion mechanism of friction enables us to understand the basic mechanism of metallic wear when a junction shears during sliding it may shear in one or other of four ways. It produced by the processes of abrasion, adhesion, erosion, tribo-chemical reaction and metal fatigue.

1.2 Introduction to bearing

Bearing is a mechanical element that permits relative motion between two parts, such as the shaft and the housing, with minimum friction.

The functions of the bearing are as follows:

- The bearing ensures free rotation of the shaft or the axle with minimum friction.
- The bearing supports the shaft or the axle and holds it in the correct position.
- The bearing takes up the forces that act on the shaft or the axle and transmits them to the frame or the foundation.

`

1.2.1. Classification of bearings

Bearings are classified in different ways, based on the direction of force:-

1) Radial bearing: These bearings support the load which is perpendicular to the axis of the shaft.
2) Thrust bearing: These are the bearing which supports the load, which acts along the axis of the shaft.

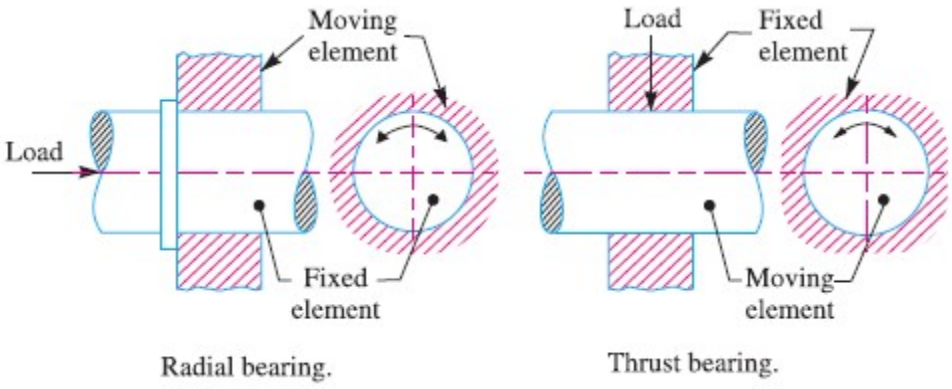

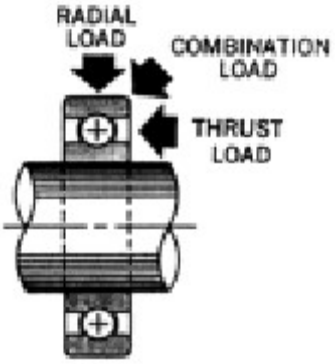

Figure 1: Radial and thrust bearings.

Bearings can be classified as hydrodynamic and hydrostatic bearings. In hydrodynamic bearings, the lubricant is absorbed or forced into the system by the rotation of the

`

bearing. Whereas in a hydrostatic bearing system, an external source like a pump is required to force the lubricant into the system.

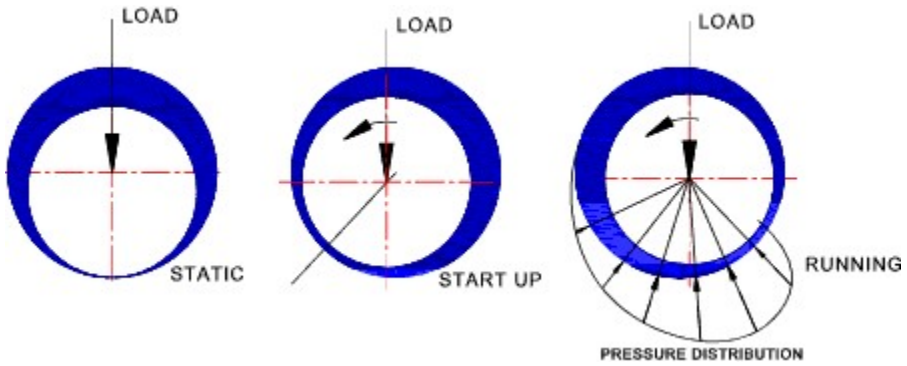

Figure 2: Hydrodynamic Lubrication

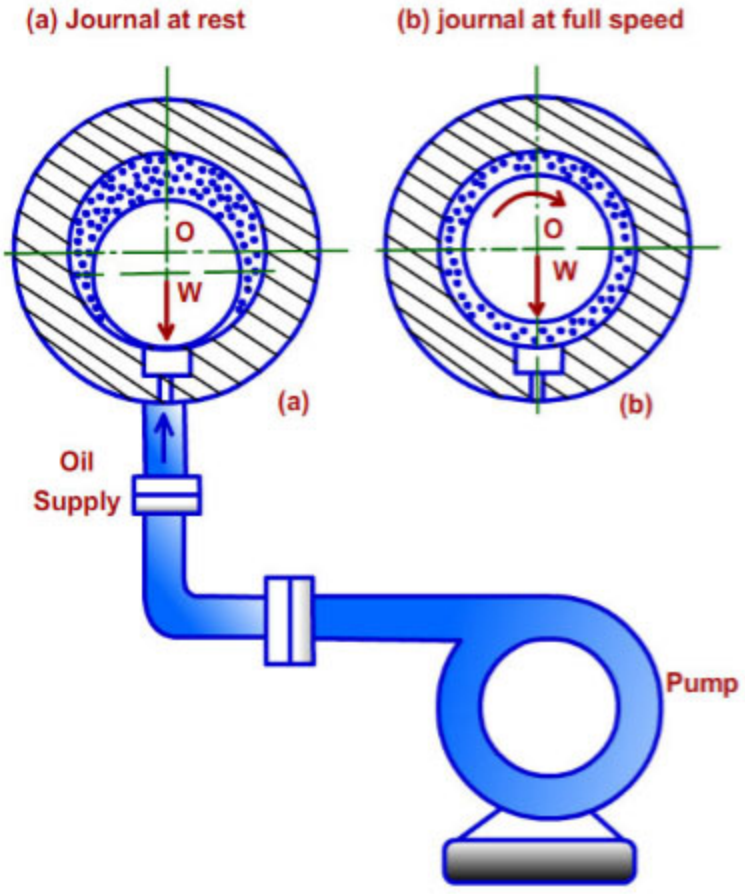

Figure 3: Hydrostatic Lubrication.

`

The most important criterion to classify the bearings is the type of friction between the shaft and the bearing surface. Depending upon the type of friction, bearings are classified into two main groups – sliding contact bearings and rolling contact bearings. Sliding contact bearings are also called plain bearings, journal bearings or sleeve bearings. A journal bearing is a sliding contact bearing working on hydrodynamic lubrication and which supports the load in the radial direction. The portion of the shaft inside the bearing is called journal and hence the name 'journal' bearing. Hydrodynamic lubrication is defined as a system of lubrication in which the load supporting fluid film is created by the shape and relative motion of the sliding surfaces.

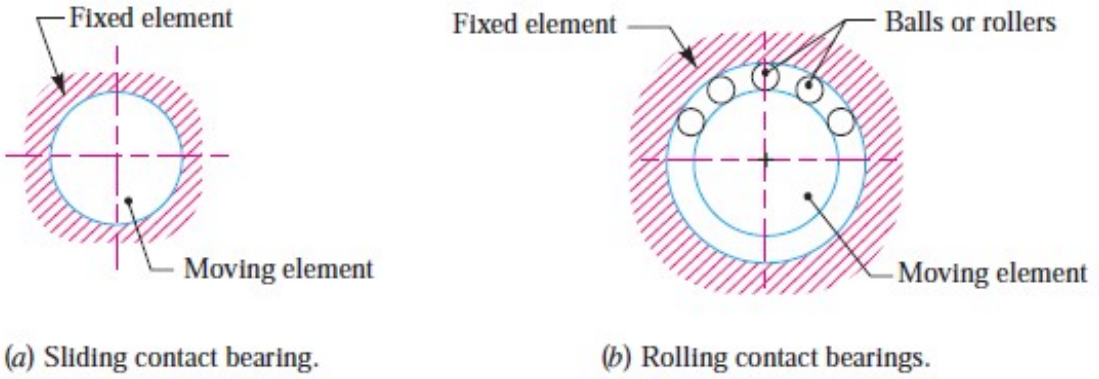

(*a*) Sliding contact bearing. (*b*) Rolling contact bearings.

Figure 4: Sliding Bearing and Roller Bearing.

There are two types of hydrodynamic journal bearings, namely, full journal bearing and partial bearing. In full journal bearing, the angle of contact of the bushing with the journal is 360°. Full journal bearing can take loads in any radial direction. Most of the bearings used in industrial applications are full journal bearings. In partial bearings, the angle of contact between the bush and the journal is always less than 180°. Most of the partial bearings in practice have 120° angle of contact. The partial bearing can take loads in only one direction. Partial bearings are used in railroad cars.

`

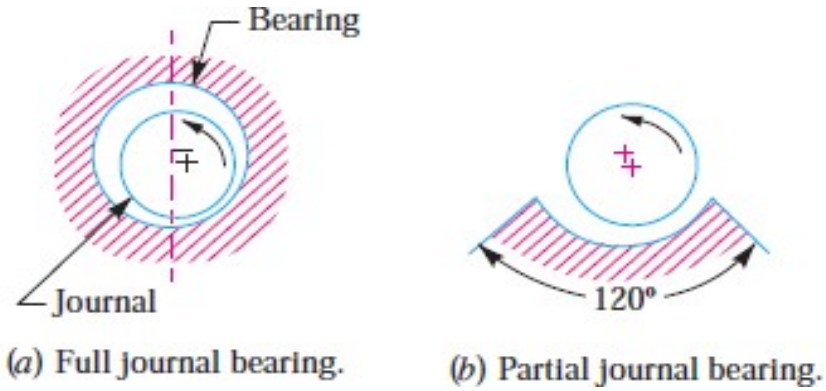

Figure 5: Full and Partial Bearings.

In this case, the surface of the shaft slides over the surface of the bush resulting in friction and wear. In order to reduce the friction, these two surfaces are separated by a film of lubrication oil. The bush is made of special bearing material like white metal or bronze. Rolling elements, such as balls or rollers, are introduced between the surfaces that are in relative motion. In this type of bearing, sliding friction is replaced by rolling friction.

In a journal bearing the metal to metal contacts depend upon the mode of lubrication or the type of lubrication. Type of lubrication means based on the extent to which the contacting surfaces are separated in a journal bearing combination. It can be classified as:

1. Thick film lubrication
2. Thin film lubrication
3. Elastohydrodynamic lubrication.

Thick film lubrication

Thick film lubrication describes as a condition of lubrication, where two surfaces of the bearing in relative motion are completely separated by a film of fluid. Since there is no metal-to-metal contact present between the two surfaces, the properties of the surface, like surface finish, have little or we can say no influence on the performance of bearing.

`

Generally, the value of film thickness is measured anywhere from 8 to 20 μm. Typical values of coefficient of friction are 0.002 to 0.010. Due to the absence of metal-to-metal contact between the two surfaces, wear is found minimum as compared to other two cases. Thick film lubrication is divided into two types hydrodynamic and hydrostatic lubrication which we had defined earlier.

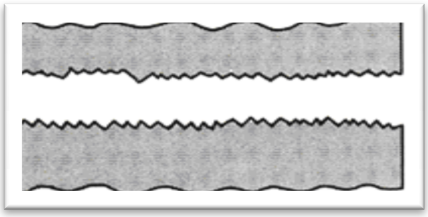

Figure 6: Thick film lubrication.

Thin film lubrication

It is also known as boundary lubrication. Here the surfaces are separated by a relatively thin film of lubricant, but at some high spots, Metal-to-metal contact does exist. Because of this intermittent contacts, it also is known as mixed film lubrication. Surface wear is mild. The coefficient of friction commonly ranges from 0.004 to 0.10.

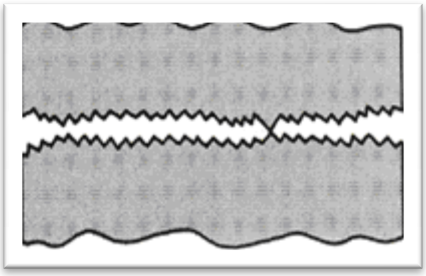

Figure 7: Thin film lubrication

`

Elastohydrodynamic lubrication

When the fluid film pressure is high and the surfaces to be separated are not sufficiently rigid, there is an elastic deformation of the contacting surfaces. This elastic deflection is useful in the formation of the fluid film in certain cases. Since the hydrodynamic film is developed due to elastic deflection of the parts, this mode of lubrication is called elastohydrodynamic lubrication. This type of lubrication occurs in gears, cams and rolling contact bearings.

In addition to this sometimes a term ‘Zero film’ bearing is also being used. Zero film bearing is a bearing which operates without any lubricant, means without any film or lubricating oil.

1.2.2. Lubricant Mechanism:

To understand the role of different regimes of lubrication Stribeck curve is used, that explain friction in journal bearing. This curve consists of the coefficient of friction (f) on the ordinate while bearing characteristics number, which is a dimensionless number, on the abscissa. The coefficient of friction is the ratio of tangential frictional force to the radial load acting on the bearing.

`

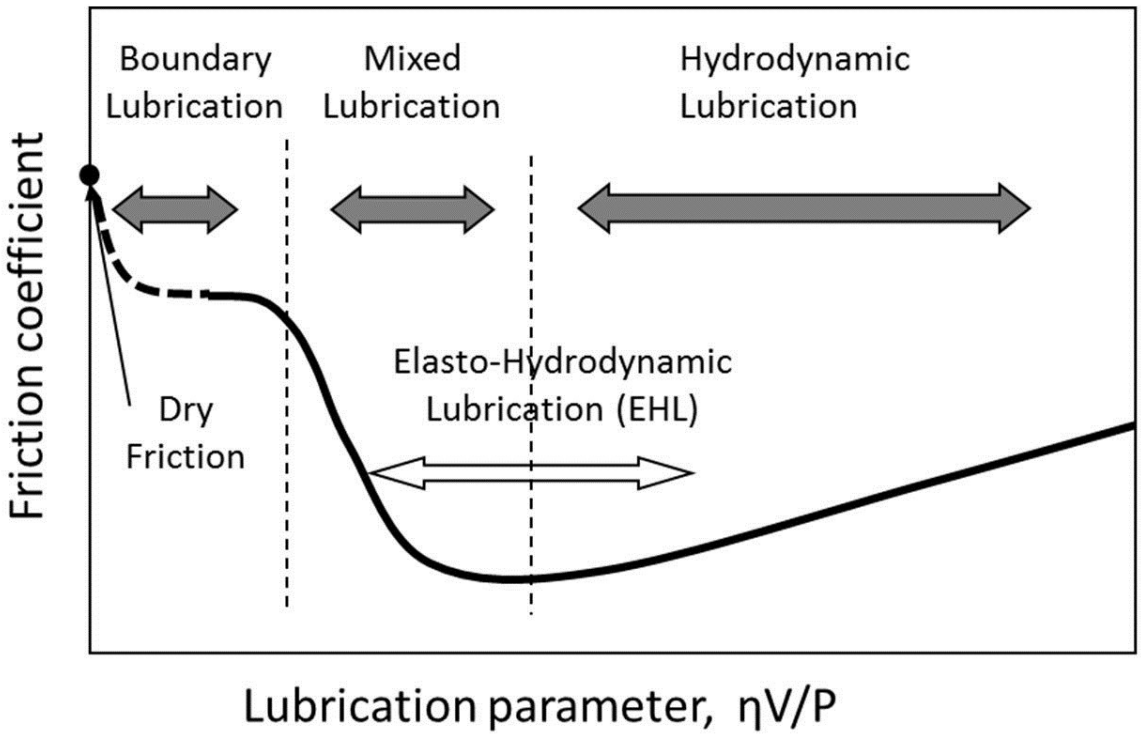

Figure 8: Stribeck Curve

The bearing characteristic number is given by the formula:

Bearing characteristic number = $\frac{\eta V}{P}$

Where, η = absolute viscosity or dynamic viscosity, Pa.s

V = speed of journal in rpm

P = bearing pressure (load per unit of projected area of bearing), Pa

From the diagram it is observed that the coefficient of friction is minimum at some point, the value of the bearing characteristic number corresponding to this point is known as bearing modulus. It is denoted by K.

`

The bearing should not be operated near the critical value k, a slight drop in the speed or a slight increase in the load will reduce the value of bearing a characteristic number which results in the formation of boundary lubrication.

It is observed from the above curve when the viscosity of the lubricant is very low, the value of the ($\frac{\eta V}{P}$) parameter will be low and boundary lubrication will form. Therefore, for a very low value of lubricant viscosity, the lubricant will not separate the surfaces of the journal and the bearing and hence metal-to-metal contact will occur resulting in excessive wear at the contacting surfaces.

This curve is important because it defines the stability of hydrodynamic journal bearings and helps to visualize the transition from boundary lubrication to thick film lubrication.

1.2.3. Journal Bearing

Journal bearing is the most common type of plain bearing. It consists of a sleeve, with a shaft rotating in it and a thin film of lubricant, restricting the contact between them. The study of journal bearing comes under Engineering Tribology. As known, small improvements in the field of Tribology leads to better use of energy.

Journal bearings are mainly used for carrying axial loads or vertical loads. Journal bearing is a hydrodynamic bearing where due to rotation of the journal in the bearing the lubricant is forced into the system. The bearing has a rotating shaft guided by a bearing, which is fixed. The friction between bearing and shaft is reduced by means of lubricants with high viscosity. The lubricant flows between the shaft and the stationary bearing. When the bearing is in running condition, there will be a pressure build up between the shaft and the bearing. The pressure should be tested for better performance and increased durability of the bearing. The principle of operation of the hydrodynamic journal bearing is:

`

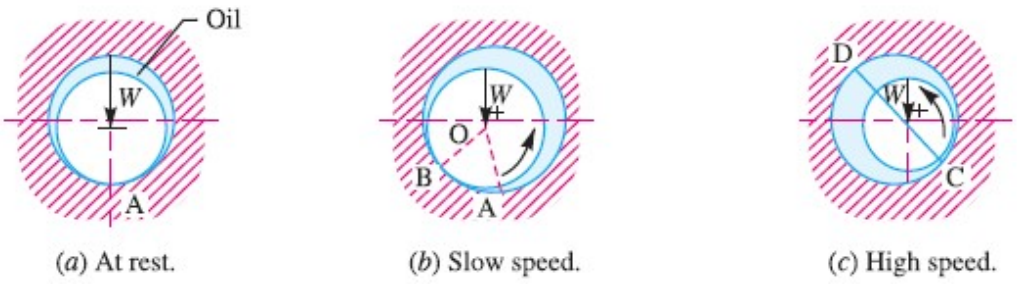

Figure 9: Different working stage of Journal Bearing.

Initially, the shaft is at rest (in fig.a) and it sinking to the bottom of the clearance space under the action of load W. The surface of the journal bearing touches the rest. As the journal bearing starts to rotate (in fig.b), it climbs the bearing surface and as the speed is further increased (in fig.c) it forces the fluid into the wedge –shaped region. Since more and more fluid is forced into the wedge –shaped clearance space pressure is generated within the system.

The pressure distribution around the periphery of the journal is shown in the figure. Since pressure is created within the system due to rotation of the shaft, this type of bearing is known as a self-acting bearing.

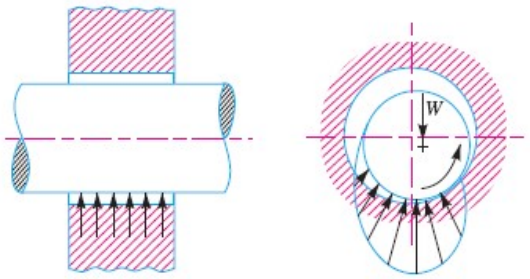

Figure 10: Oil Pressure Distribution in Journal Bearing.

A Test Rig is an apparatus or equipment used for measuring the performance of any mechanical equipment. Test Rig can be placed in the laboratory for studying pressure distribution of the journal bearing.

`

Journal bearing play an important role in almost every automobile application. The bearing guiding the shaft should have good thermal properties, strength, and load bearing capacity.

1.2.4. Applications of bearing:

Sliding contact (journal) bearings are used in the following applications-

i. Crankshaft bearings in petrol and diesel engines;
ii. Centrifugal pumps;
iii. Large size electric motors;
iv. Steam and gas turbines;
v. Compressors; and
vi. Concrete mixers, rope conveyors, and marine installations.

Rolling contact bearings are used in the following applications-

i. Machine tool spindles;
ii. Automobile front and rear axles;
iii. Gearboxes;
iv. Small size electric motors; and
v. Rope sheaves, crane hooks, and hoisting drums.

1.3 Brief introduction to the software used

1.3.1. MATLAB

MATLAB is an object-oriented high-level interactive software package for scientific and engineering numerical computations. Its name stands for *matrix laboratory*. MATLAB enables easy manipulation of the matrix and other computations without the need for traditional programming. MATLAB's basic data element is the matrix.

`

History

Cleve Moler, the chairman of the computer science department at the University of New Mexico, started developing MATLAB in the late 1970s. He designed it to give his students access to LINPACK and EISPACK without them having to learn Fortran. It soon spread to other universities and found a strong audience within the applied mathematics community. Jack Little, an engineer, was exposed to it during a visit Moler made to Stanford University in 1983. Recognizing its commercial potential, he joined with Moler and Steve Bangert. They rewrote MATLAB in C and founded MathWorks in 1984 to continue its development. These rewritten libraries were known as JACKPAC. In 2000, MATLAB was rewritten to use a newer set of libraries for matrix manipulation, LAPACK.

MATLAB was first adopted by researchers and practitioners in control engineering, Little's specialty, but quickly spread to many other domains. It is now also used in education, in particular, the teaching of linear algebra, numerical analysis, and is popular amongst scientists involved in image processing Graphics and graphical user interface programming.

MATLAB supports developing applications with graphical user interface (GUI) features. MATLAB includes GUIDE (GUI development environment) for graphically designing GUIs.It also has tightly integrated graph-plotting features. For example, the function *plot* can be used to produce a graph from two vectors *x* and *y*.

`

Chapter 2

LITERATURE REVIEW

Kornaev et al. [1], had developed the lubricant's sample by means of adding the fullerene black, fullerenes, molybdenum disulfide, and fluoropolymer in quantity no higher than 0.05% of the mass in base low-viscosity mineral oil. The experiment was made during the run-down of the rotor, and they measured the friction coefficient in the journal bearing and the vibrations of its housing. They found that ultrafine additives significantly decreased the load-carrying capacity and the friction coefficient in the journal bearing, as well as the vibration level in the bearing. The rate of lowering of friction and vibration directly depended on the level of pseudoplastic properties of the sample. The best results were shown by samples with fullerene black and fluoropolymer.

The experimental study of the properties of the lubricant samples was conducted under the condition of fluid-film bearing lubrication during the run-down of the rotor. The effect of simultaneous decrease of the friction coefficient and level of vibration was observed when the bearing was lubricated with samples with ultrafine additives. This effect was mainly shown in the case of samples with fluoropolymers, fullerene black, and fullerene. Theoretically, the decrease of the friction coefficient by 15–25% is explained by the decrease of the viscosity of pseudoplastic fluids at high rotor speeds, as well as by the decrease in the load carrying capacity and by thinning of the lubricant's layer. In such state, unlike Newtonian fluids, pseudoplastic fluids enhance their dynamic properties and help significantly decrease the vibrations level in journal bearings. The level of vibrations of the bearing's housing when going through the resonance zone of the test rig, decreased by 1.5 times.

On the basis of the implemented research, it can be concluded, that the application of the lubricant with ultrafine additives (fluoropolymer, fullerene black or fullerenes) allows

`

simultaneously significantly lowering the friction loss and enhancing the damping capacity of the journal bearings.

Cheng and Wei xi Ji [2], have developed a velocity-slip model for analysis of the fluid film in a journal bearing, including slip length within the cavitation region and slip boundary conditions at the gas-liquid interfaces, and well predicts the load capacity.

In their analysis, they found that at a lower rotating speed of the rotor, the slip effects within the cavitation region can increase the static load capacity as well as the direct stiffness coefficient of a journal bearing but decrease the damping coefficients and the critical mass of the journal bearing.

High slip coefficient (Ks¼1) and bubble concentration (β¼100%) can form in divergent region of the journal bearing; while for a higher rotating speed, the slip effects within the cavitation region have no influence on the static and dynamic characteristics of the journal bearing as well as the critical mass of the journal bearing.

Sun et al. [6], investigated that shaft deformation under load will cause journal misalignment in shaft-journal bearing systems.

They found that oil film pressure, oil film thickness, and oil temperature at corresponding positions of two sections, symmetric with respect to the central section of the bearing, are different when their journal misalignment occurs due to the shaft deformation. Their experiment showed the differences of the values of the maximum film pressure, the minimum film thickness, and average film temperature at the two end sections symmetric about the central section of the bearing increase with shaft load, and the angle of journal misalignment results from increased shaft deformation.

It was also observed that the smaller the ratio of radial clearance cc to length LL of a bearing, the more obvious the effect of journal misalignment becomes stemming from

`

shaft deformation, and affecting the values and distributions of oil film pressure, oil film thickness and oil film temperature in a journal bearing.

Wang et al. [8], studied the behavior of mixed lubrication on finite journal bearings operating under steady state conditions with large eccentricity ratios. It can be concluded that Elastic deformation, the surface roughness effect on lubrication and asperity contact pressure are the three major factors influencing journal bearing performance. These factors must be taken into account for accurate modeling of the mixed lubrication process. 1. The maximum asperity contact pressure always occurred at the bearing edges of the finite bearing structure used in this study. 2. The distributions of the asperity contact pressure and the contact area are strongly influenced by the bearing width, surface roughness orientation, load, and journal speed. 3. The transverse surface roughness orientation enhances the hydrodynamic lubricating action of the journal bearings and increases the film thickness for cases where LID = |. The advantages of having transverse roughness disappear when LID = i.

Baskar et al. [3], conducted an experiment and found that with the use of a biolubricant (CMRO) the friction coefficient was high, whereas the addition of nano-CuO to CMRO reduces the friction coefficient significantly. Higher wear related to severe pits and deep cavities on the bearing surfaces was noticed with the use of CMRO than with the synthetic lubricant. Improved wear reduction behavior could be attributed to the formation of a tribofilm on the wear tracks by a biolubricant with nano-CuO. It was observed that the Nano-CuO is the best suitable anti-wear additive for the biolubricant among the selected nano additives.

This investigation was only to determine the influence of biolubricants with nano additives on a typical journal bearing system. It can be concluded that CMRO with nano CuO as an anti-wear additive is the best suitable biolubricant candidate for the

`

replacement of a synthetic lubricant which can reduce the dependence on petroleum-based products, and which is also environment-friendly.

Feng et al. [17], conducted an experiment on Analysis of novel hybrid bump-metal mesh foil bearings. They developed a theoretical model of Hybrid bump-metal mesh foil bearings (HB–MFBs) and performs a numerical analysis of foil structure and MMBs to predict bearing performance. They found that the foil strip adds several circular bumps between adjacent trapeziform bumps along the bearing circumference, hence by avoiding excessive sagging between two supporting points it can be reduced.

It was also found that the bearing temperature increases from ambient temperature when the rotor starts to spin, this trend maintains for a certain period and then stabilizes in the last operation. Hence the total temperature increases slightly, which indicates the full gas film lubrication of the test bearing. Also the predicted minimum film thickness at the bearing midplane increases along with rotational speed, but rapidly decreases with an increasing applied load. High mesh density also leads to low minimum film thickness.

The compliance of HB–MFBs enable the journal eccentricity to exceed the nominal radial clearance for a heavy load. The predicted results show that the mesh density significantly affects the bearing dynamic force coefficients, particularly at low rotational speeds. The bearing stability analysis which considers the Coulomb friction of the test bearing reveals that the friction inside the MMBs can increase the critical mass and bearing stability. The Coulomb friction coefficient which determines the bearing damping coefficients increases the critical mass non-linearly along with an increasing bearing load. The mesh density also significantly influences the bearing stability. The increment of the critical mass of high mesh density is larger than that of the critical mass of low mesh density.

`

Ighil and Fillon [19], investigated numerically thermal and surface texturing effects on the journal bearings. On the basis of their investigation the following conclusion can be drawn:

i. It is not necessary that texturing over the entire bearing surface improve the hydrodynamic characteristics (friction reduction, increase of the minimum thickness of the fluid film, improvement of hydrodynamic lift effect and others) in a journal bearing contact.

ii. For very low journal rotational speeds and adequate dimple sizes, fully textured can lead to some significant positive effects (up to +27% of minimum film thickness increase and up to -3.4% friction coefficient reduction).

iii. Partially texturing at the outlet of the active pressure zone has always a positive effect, for average and high rotational speed. This result is due to the improvement of the active fluid film region that allows a better distribution of the pressure and contributes to the enhancement of the contact loading capacity.

iv. The main criterion for enhancement of journal bearing performance is texture arrangement, mainly the location domain on the journal bearing. The type of dimples and their geometrical characteristics have also a great influence on the bearing performance improvement.

v. It was observed that the selection of optimal dimple shape and sizes, when the journal bearing is operating at low speeds (speeds lower than 500 rpm), put dimples in the bearing first angular part (between 0 and 180°) which the maximum pressure region is. On the other hand, the performances of the journal bearing operating at high speeds can always be improved by texturing the bearing second half part (beyond180°), at the pressure curve declining part.

Kun Li et al. [27], identified the oil-film coefficients for a rotor-journal bearing system based on equivalent dynamic load reconstruction and measures the equivalent loads, oil-film stiffness and damping coefficients using the least square method. They identified the

`

oil-film characteristic coefficients, which plays a very important role in monitoring and maintaining the stable work of the rotor-journal bearing system.
For well reconstructed oil-film loads, they used the weighted residual integration method based on the least squares, to identify the oil-film coefficients, which comprehensively utilize the information of the reconstructed loads and calculated unbalance responses in the time domain.

Nacer and Michel [34], found recessed and non-recessed journal bearings are used in various engineering applications because of their good performance over a wide range of speed and load, besides their relative simplicity in manufacturing. However, a non-recessed hybrid journal bearing gives better performance over the recessed/pocketed hybrid journal bearing, such as improved load-carrying capacity at low and high speeds, low power consumption, increased minimum fluid-film thickness, large fluid-film damping and relative simplicity in manufacturing.

The effect of surface texture in the form of the elliptical-shape dimples with various depths, diameters, area ratios and different operation parameters on friction coefficient has been evaluated by **Chenbo and Hua [33]**, under conditions of hydrodynamic lubrication. The Reynolds boundary condition is adopted to take the cavitations into consideration. The Reynolds equation, with its appropriate boundary conditions, was solved by a finite difference method where a dense grid is applied within the dimple area.

One-dimensional analysis of partially textured slip slider and journal bearing has been done by **Rao et al [17]**. Partially textured slip followed by a single groove is considered on the stationary surface of slider and journal bearing. A modified Reynolds equation is obtained. The non-dimensional pressure and shear stress expressions are derived for (i) partially textured slip convergent slider bearing, (ii) partially textured slip parallel slider

`

bearing, (iii) partially textured slip convergent journal bearing, and (iv) partially textured slip concentric journal bearing. Reynolds boundary conditions are used to solve the pressure distribution in the convergent journal bearing. In this work, the influence of partially textured slip configuration on the generation of load and consequent reduction in friction is analyzed.

The compound dimple also has positive effects on the tribological performances of the journal bearing. The tribological performances for the bearing with the compound dimple and simple dimple are studied by **Meng et al. [35]**, using a fluid structure interaction (FSI) method. Numerical results show that the compound dimple can supply the larger load-carrying capacity and lower friction coefficient due to its twice hydrodynamic action in comparison with the simple dimple. Moreover, the above improvement depends on the geometry sizes of the compound dimple, the dimple interval, and working parameters of the bearing.

Ahmad et al. [36], performed an experimental work to determine the effect of oil groove location on the temperature and pressure in hydrodynamic journal bearings. A journal with a diameter of 100 mm and a length-to-diameter ratio of 0.5 was used. The oil supply pressure was set at 0.20–0.25 MPa. The groove was positioned at seven different locations, namely -45^{o}, -30^{o}, -15^{o}, 0^{o}, +15^{o}, +30^{o} and +45^{o}. Measurements of temperature and pressure were obtained for speeds of 300, 500 and 800 rpm at different radial loads. Changes in oil groove location were shown to affect the temperature and pressure to some extent.

Brito et al. [37], performed an experimental assessment of a journal bearing with either one or two axial grooves located perpendicularly to the load line. It was found that under heavy loaded operation the twin groove configuration might actually deteriorate the

`

bearing performance when compared with the single groove arrangement, namely due to uneven lubricant feed through each groove. It was concluded by authors that the knowledge of the feed flow rates through each groove can be used to improve bearing performance under specific regimes by implementing groove deactivation or flow balancing strategies.

Christensen and Tonder [38], studied the effects of roughness on the bearing characteristics of a full journal bearing of finite width. This hydrodynamic theory of lubrication of rough bearing surface which considered the film thickness in the bearing as a stochastic process. A Reynolds-type equation was developed which was similar to the equation for smooth surfaces. The results showed a small change in the functional characteristics of a journal bearing due to surface roughness in most of the cases. The effects depend upon the nominal geometry and operating conditions. Therefore for the analysis of a general bearing including the effects of roughness the ordinary Reynolds equations can be used.

Wang et al. [39], studied the phenomenon of mixed lubrication in a finite journal bearing having large eccentricity ratios. This study was based on the combined effects of bearing deformation, surface roughness, and asperity interactions. In this study, they utilized the average Reynolds equation to analyze the effects of surface roughness on lubricant flow. The FEM-based influence-function method was considered to calculate the deformations under hydrodynamic pressures. The results showed that the maximum average pressure, corresponding to the highest eccentricity ratio was approximately 40 MPa at 1500 rpm. In most of the cases, the journal bearing was operating under mixed lubrication regime without any seizure.

Vijayaraghavan and Brewe [40], studied the rate of viscosity variation on the performance of journal bearing. In this study, they utilized the Roeland model on viscosity-temperature-pressure which characterizes the viscosity profile of a lubricant

`

when viscosity values are known corresponding to two unique temperatures and pressures. To incorporate the cavitation effects and distribution of fluid properties across film thickness, THD numerical model was used. A high viscosity lubricant was used for the study and performance parameters and pressure distribution is determined. The results showed that the effects of rate of viscosity variation are diminished if the lubricant supply temperature is lower than the temperature at which the viscosity of the lubricants is same.

Poddar and Tandon [41], experimentally studied the vapour cavitation of journal bearing using vibration, acoustic emission and oil film photography. Their set-up consisted of a journal bearing rig with transparent sleeve, a bronze bearing insert and LED illuminator. Their study found the cavitation to be of vaporous type. The acoustic emission results confirmed the occurrence of vapour cavitation due to the generation of elastic transient wave. From the vibration results it was found that the vapour cavitation played a significant role in dampening of rotor vibrations.

Santos et al. [42], studied hydrodynamic journal bearing by applying the ideas in Generalized Integral Transform Technique to solve the Reynolds equation. This approach is an Eigen function expansion methodology for solving multiphysics problems. Extensive parametric analysis is done and the results are compared with the GITT approach to show its consistency. The GITT approach was successfully employed in the analysis and can be extended to take into account the dynamic cavitation, bearing deformations and heat exchange.

Harnoy [43], develops an analysis for the time-variable friction during the start-up of a journal in a lubricated-sleeve bearing. A dynamic friction model has been developed from the theory of unsteady lubrication. A stribeck curve is also developed between the friction vs. Steady velocity and hysteresis curve is obtained in case of oscillating velocity.

`

The result shows that friction can be reduced by high start-up acceleration. A reduction in the maximum friction force and friction energy losses is obtained when bearing support is flexible. High start-up acceleration can't be achieved in every bearing. This paper indicates various alternatives to increase the torsional stiffness of the shaft which provides flexible bearing support.

Christensen and Tonder [44], describes the application of hydrodynamic theory of lubrication of rough bearing surfaces. The analysis of a full journal bearing (with finite width) is done with the help of this theory. This paper mainly focuses on how the roughness influences the characteristics of the bearing and corresponding bearing response is obtained. The result shows that the effect of surface roughness on the characteristics of a journal bearing is small in most cases. The result of this experiment agrees with the hydrodynamic theory of lubrication of rough bearing surfaces. Near the hydrodynamic limit roughness shows an appreciable effect. Expression is obtained from Reynolds's equation.

Tzeng and Saibel [45], studied the effect of roughness of the surfaces of a journal bearing on the pressure development, load carrying capacity, attitude and friction. In this, surface roughness is treated as a random quantity which is characterized by a probability density function which can be determined experimentally. A numerical example is also given which shows that an increase of the loading capacity occurs when the roughness of the surface is taken into account. The friction force increases but less significantly than the loading capacity. Hence, a very smooth surface leads to a less satisfactory bearing from the hydrodynamic point of view.

Gengyuan et al. [46], develops a numerical analysis to design a good journal bearing having water as a lubricant. The effects of eccentricity ratio on pressure distribution of

`

water film are analysed by CFD. Numerical analysis is developed with different dimensions and rotational speeds of a journal bearing. This provides a reference for selecting the initial dimension which helps in designing a perfect water lubricated bearing for given load and rotational speed. Eccentricity ratio is considered as an important factor for improving hydrodynamic performances of plain journal bearings.

Tsai and Jeng [47], analyses the performance of hydrodynamic journal bearing by applying journal bearing method to solve the average lubrication equation for grain flow. They have investigated various issues like the grain characteristics, including the particle size and the grain-grain collision elasticity. The non-dimensional load, attitude angle, friction coefficient, and side flow are explored for different eccentricity and diameter-to-width ratios. The numerical values are useful to provide the performance of powder lubricated journal bearing. In last the experimental values are compared with numerical values and results are found satisfactory.

Soto et al. [48], studied the design process of journal bearing of turbo machinery, which is very complex and time consuming due to the many geometrical and physical variables involved. This study reports on design of experiments (DOE) and the response surface design of experiments (RSDOP) methods works on the design of the drive-end and free-end three load journal bearings supporting a centrifugal rotor. The advantages and disadvantages of each technique are discussed. The bearing design variables are bearing slenderness ratio, radial clearance, and preload and lubricant inlet temperature. The rotor dynamic response variables selected were the critical speed location, the vibrations at critical speed and operating speed for both bearings, and the threshold speed of instability. An optimization approach combining an SRDOE and rotor dynamic finite element modelling is presented.

`

Stolarski et al. [49], conducted an experiment on an acoustic journal bearing and shows that the overall shape of the bearing and geometry effect for the load capacity of the bearing. On the basis of their experiment following conclusion can be withdraw:

i. It was found that journal air bearing operates on a squeeze film acoustic levitation principle.
ii. For a load supporting capacity of a acoustic bearing, geometric configuration plays an important role.
iii. Results shows increased flexibility of the bearing directly translates into bigger elastic deformation amplitude of the initially circular bore which helps in improving the ability to separate the interacting surfaces. This thing is only valid with the assumption that the force generated by PZT and responsible for elastic deformation of the bearing is kept constant.

Dadouche and Conlon [52], has investigated the effect of surface texturing on the steady-state performance characteristics of highly-loaded journal bearings lubricated with a contaminated lubricant (as hydrodynamic journal bearings has serious performance issues due to contamination from moisture, foreign particles, dust and wear debris). It was found that:

- Bronze journal bearings can tolerate a considerable amount of hard particle contaminants as long as the size of the particles is lower than the minimum film thickness and the bearing runs with minimal misalignment.
- Hard particle presence in bearing lubrication system generates a much higher vibration level which is a sign of possible performance issues.
- Highly textured journal bearings (~15% pit area) showed positive results in terms of contaminant ingestion compared to plain smooth surface journal bearings.
- Tighter manufacturing tolerances combined with light surface texturing may result in better contaminant allowance in bearing lubrication systems with a penalty of higher operating temperatures and increased power losses within the bearing.

`

Ren and Feng [58], has investigated the stability of the step recessed, hydro-static and -dynamic hybrid water-lubricated journal bearings for fuel cell vehicle compressor.
It is observed that the OB (one has an orifice in each deeper recess), has better stability under high operating speed and low supply pressure, while the GB (one has a circumferential central groove whose depth is much bigger than the recesses) is more suitable for low operating speed and high supply pressure condition. The water supply pressure increases the direct stiffness and damping of the bearing, and then improves the bearing stability. The turbulence can improve the stability under large Sommerfled number condition.

Miyanaga and Tomioka [62], investigated the effect of support stiffness and damping on the stability characteristics of the herringbone-grooved aerodynamic journal bearings with viscoelastic supports. They conducted the experiment to clarify the effect of support stiffness and damping on the stability characteristics of the bearings. To examine the various viscoelastic support conditions the linear perturbation analysis and the non linear transient analysis are used. It was observed that the groove configuration that gives the highest threshold speed of whirl changes with the viscoelastic support conditions. It was also observed that there is a possibility to stabilize the bearings by viscoelastic supports. However, the threshold speed for lower damping support conditions decreases rather than that for rigid support condition.

Machado and Cavalca [66], approached experimently to evaluate a wear model for hydrodynamic cylindrical bearings. This paper brings contributions to the analysis of the cylindrical hydrodynamic bearing wear influence on the behavior of the rotating system. Therefore, a mathematical model is used to represent the wear on these bearings, and s

`

procedure is proposed to estimate the wear main parameters from the dynamic response of the rotor-bearing system. The wear model and the estimation process are promising in representing the worn bearings in rotating systems and consequently, in the application to identify the wear parameters. The directional response was sensitive to the wear model and, therefore, consolidated the purpose of its use in the objective function of the searching process. Wherein the identification is focused in the backward component of the response, bearings with more symmetrical, or isotropic characteristics promising most sensitivity to the model, once the identification in anisotropic bearings, such as cylindrical plain bearings, is more challenging in this case. An experimental apparatus was assembled to measure the dynamic response of the system. The results obtained from the experimental tests showed that the search method was robust enough to identify the parameters of different wear patterns, indicating that the wear model as well as the search method showed efficiency in performing their respective functions. Therefore, the feasibility of a model to identify the wear parameters in lubricated bearings was satisfactorily achieved, contributing to the studies related to the identification of wear in hydrodynamic bearings. Moreover, most of the wear iden- tification methods available in literature are based on direct measurements of the bearings characteristics, such as pressure distribution, *Locus* of the shaft, the Sommerfeld number, etc. The advantage of the method proposed in this paper is to use vibration measurements, to access the information necessary to bearings, directly on the rotor, a more accessible procedure for application in real systems. Furthermore, the using of the system response in the frequency domain enables the use of standardized tests, such as certified stability tests from API in order to identify the wear parameters.

Synnegård et al. [73],This paper evaluates how cross-coupling coefficients affects the dynamics of a vertical rotor with tilting pad journal bearings. For vertical machines, the bearing properties are dependent on the bearing load and direction. As a result, it generally requires that bearing properties are calculated at each time step using the governing fluid dynamic equations. This method gives a good representation of the

`

bearing but computational time increases and can cause stability problems. It is investigated for horizontal machines where the working point is influenced by the dead weight of the rotor, the ratio between the direct-and cross-coupling stiffness is high and the cross-coupling could be neglected. For the vertical machine investigated in this paper, the stiffness in the direct direction is only around 5 times larger than the cross-coupling at the extreme case. This does not effect the displacement to a large extent, however the force in the bearing is affected.

Choe et al [75], has studied the endurance performance of composite journal bearings under the oil cut situation. In this work, composite journal bearings were fabricated using a carbon-fiber/phenol composite and carbon-fiber/epoxy composite to solve the seizure problem of a metallic journal bearing under the oil cut situation. Friction coefficients of two composite materials were measured through the wear test under the same conditions as the oil cut situation, and the material properties were measured at the elevated temperature of the oil cut situation. Next, the stress distribution of the composite journal bearings was investigated by using finite element analysis (FEA) with respect to the friction coefficients between the rotor and bearing, and the Tsai-Wu failure index was calculated to investigate the possibility of failure.To verify the failure analysis results, the oil cut tests for the composite journal bearings were conducted using the industrial test bench. The oil cut test results indicate that the carbon fiber/epoxy composite journal bearing is more durable than the carbon fiber/phenol composite journal bearing. The following conclusion can be derived:

1) The material strengths, particularly the ILSS, for the carbon/phenol composite were substantially decreased at 150 _C; alternatively, the strengths of the carbon/epoxy composite were only slightly decreased at 150 _C because of its high glass transition temperature, Tg.
2) The carbon/phenol composite exhibited a lower friction coefficient than the carbon/epoxy composite.

`

3) In the case of the failure index calculated with the material strengths at 25 _C and 150 _C, the failure index of the carbon/phenol composite bearing exceeded 1 for all friction coefficients.
4) The failure index of the carbon/epoxy composite bearing did not exceed 1 for all friction coefficients, regardless of the material strengths at 25 _C and 150 _C.
5) The carbon/epoxy composite bearing withstood for 285% longer than the carbon/phenol composite bearing during the oil cut test. For the carbon/phenol composite bearing, serious heat deterioration of the composite material was observed after the undue wear and delamination, and wear debris was generated. The carbon/epoxy composite bearing exhibited smooth abrasive wear.

`

Chapter 3
EXPERIMENTAL SETUP

The journal bearing rigTR-660 is used to demonstrate the pressure distribution inside bearing. It is a sturdy versatile apparatus, easy to operate with provision to measure pressure at a different angular position on the bottom half of journal bearing. The journal is mounted horizontally on a shaft supported on self-aligned bearings, the shaft is rotated with by a motor with timer belt. A loaded bronze flawless bearing freely slides over the journal and as it rotates bearing is formed, radial load is applied on bearing by pulling it upwards against journal by a loading lever. 10 sensors are fixed on the circumference of bearing with their terminal ends ending in the junction box. The journal is driven by belt & two step pulley arrangement and speed required is set on software. Radial load & journal speed are varied to suit the test conditions.

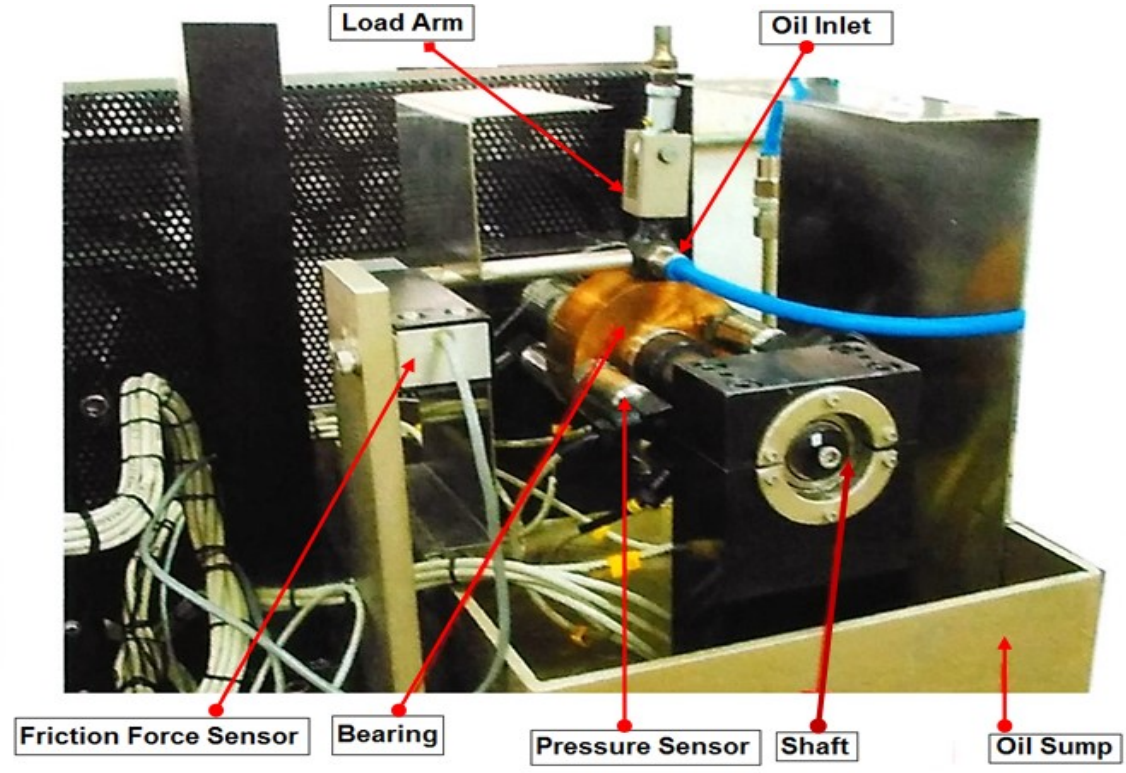

Figure 11: Journal Bearing Test Rig TR-660

`

All test assemblies are mounted on a base plate of the structure mounted on 4 no's of anti vibration pads, these pads initially used to level machine using a spirit level and later while testing absorbs vibration produced during test & prevents floor vibration transferred to equipment. The structure sides are covered with panels, on one side panel all electrical sockets are fitted.

A ground 22±0.005mm shaft is supported on two self-aligned bearings on either end of the oil sump. The oil sump is wide enough to house the bearing with all sensors with the connector inside it, a gradient taper at the bottom surface of oil tank directs the used oil into the drain pipe, the drain pipe is connected to lube unit for re-circulation of oil. A T-joint is provided on drain pipe to discharge oil into a beaker for measuring oil discharge. On one end of the shaft, a driven two step pulley is fixed, the shaft is rotated by a motor with timer belt arrangement. To attain a low speed of 40 rpm & max speed of 8000rpm two step pulley's having ratio of 1:4 & 4:1 ratio is fixed on shaft & motor ends. The shaft is driven by a motor having base speed of 1435 rpm, it is mounted on the base plate.

A journal slides over the shaft and held in position by two bush holders tightened by grub screws, the positive drive to the journal is through the key way on shaft, the tolerance on journal is controller to give minimum run out on journal. When different radial clearances are required for conducting tests, change only the journal. On this equipment a journal having 40.005mm outer dia is fixed to give c/r ratio of 0.00135mm, the outer dia of journal is ground to have surface finish of 1.6 Ra value.

Figure 12: Bearing

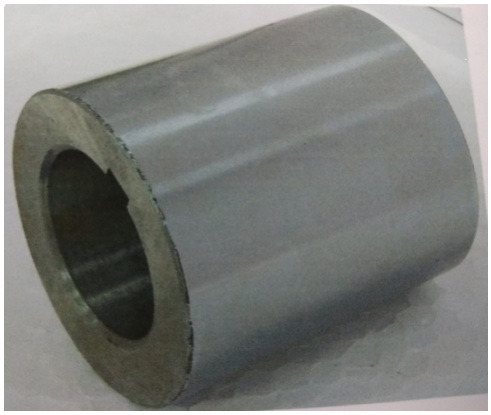

Figure 13: Journal

`

A leaded bronze bearing having l/d ratio=1 slides over journal with radial clearance of 0.0027mm. The inner surface of bearing is grounded & polished to surface finish of 1.6Ra value with cylindricity & roundness below 3 microns (the id of bearing 40.06mm). On either faces of bearing 5 no's of sensors are mounted to measure pressure at different angles, the cable ends from these connectors terminate on a junction box fixed on base plate. Radial load on bearing is applied by lifting the bracket through a wire rope, two ball bearings fixed 120° apart applies at bottom of bracket applies load on the bearing. The oil for test is supplied through top port into bearing, a rectangular cut out on inner dia of bearing retains a portion of oil to prevent oil starvation during test. A rod projects from the load cell to press against the oil inlet to measure frictional force.

A loading lever having 1:5 loading ratio is fixed on a frame, the frame height is kept sufficiently high to minimize the reduction of radial load due to inclination of loading lever when max weight is placed. The loading lever is pivoted to a vertical frame, smaller end of lever is connected to bearing top through a wire rope, on either ends of wire spherical eye bolt is fixed to give free angular movements.

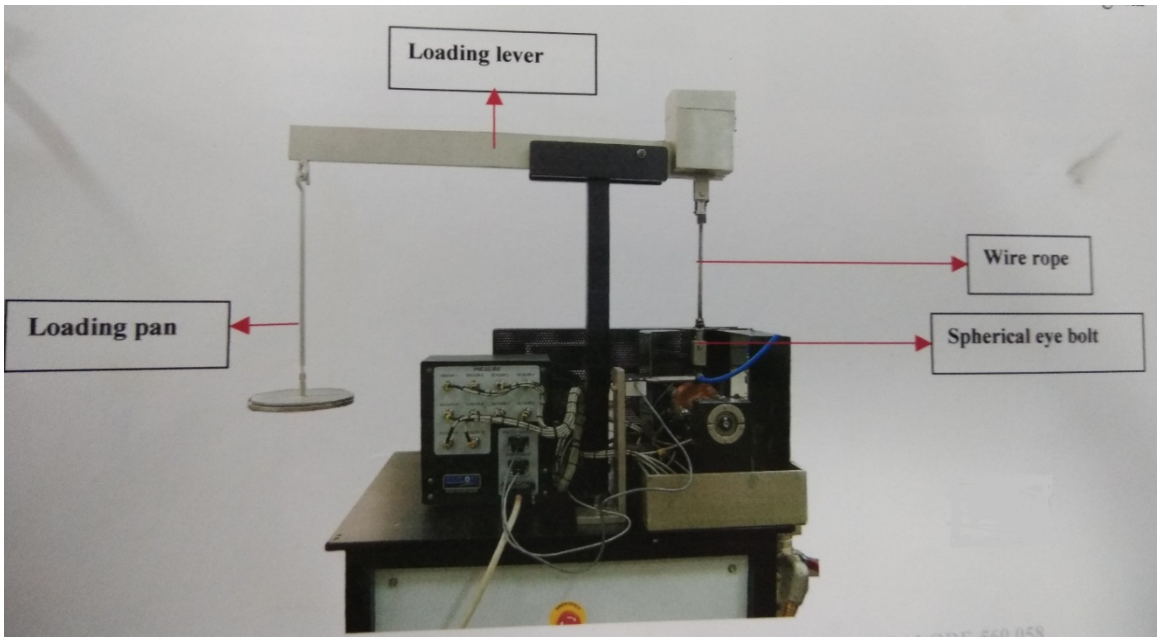

Figure 14: Complete Experimental Setup.

`

Temperature sensor :

One PT-100 temperature sensor is fixed to oil inlet above bearing to measure oil temperature before entering bearing.

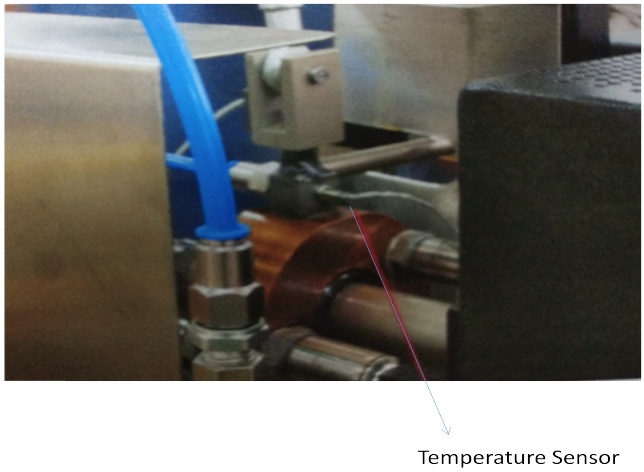

Figure 15: Temperature Sensor

Pressure sensor:

10 no's of digital stainless steel pressure sensors are fitted on either faces of bearing it can measure pressure of oil 10 MPa or 1450psi, it is fitted to bearing with BSP ¼", 1mm holes connects bearing inner dia. to pressure sensors, during rotation oil is pushed through this hole on to sensor to measure pressure. The sensor is mounted on the following position in bearing.

Figure 16: Pressure Sensor

`

Frictional Torque sensor :

Beam type load cell 30 kg capacity is fixed on to oil sump; the frictional arm touches the oil inlet projecting from bearing. During journal rotation the force exerted is transferred to load cell, it is measured and displayed on PC screen. The torque distance is 51mm.

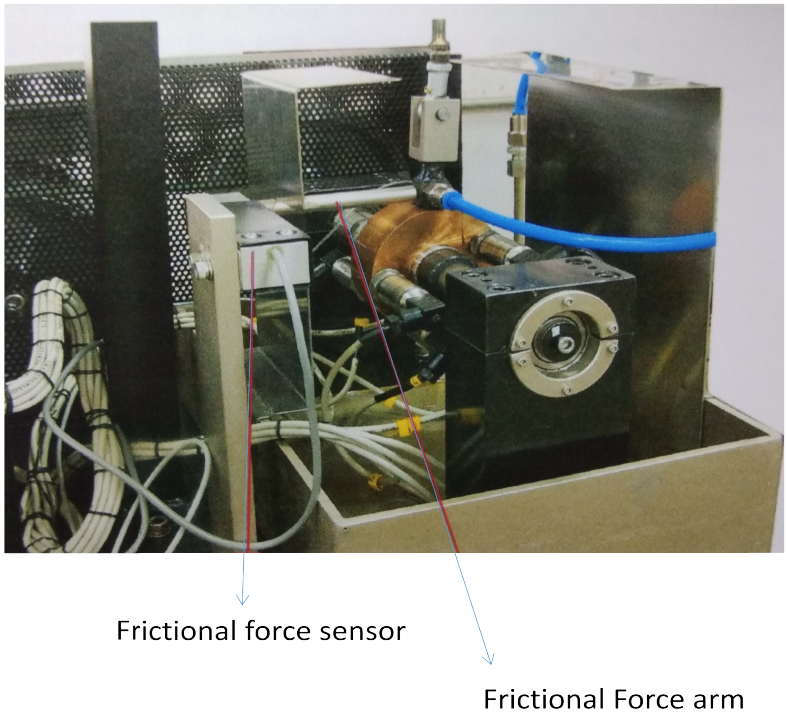

Figure 17: Frictional Torque sensor

Electrical controller

The controller box is positioned near machine for easy handling, it houses PCB's & other electrical items. The power supply to motor & pneumatic system is from controller. The sensor terminal ends are connected to the instrumentation card fitted inside the controller.

Cables

- **Power input cable:** To transfer 415V, 3 phase, 50 Hz, 10A power from customer site to machine. A 5 core, 2 meter cable of 1.5mm square is to be connected to machine end with BCH plug and other end is kept free suitable for fitting into socket at customer end.

`

- **19 pin control cable:** The cable has two 19 pin MS connector on either ends to transfer power & signal from machine to controller.
- **Signal input cable:** The cable has two 15 pin D type connectors fixed on either ends of cable to transfer signal from sensors to controller.
- **NI cable:** It connects controller to PC.

3.1 Specification of journal bearing rig TR-660

Table 1: specification of machine

S.No.	Test Parameters	Details
1	Pressure	Digital Pressure Sensor
2	Friction Factor	
3	Oil Flow Rate	
4	Temperature of Inlet of Bearing	Thermocouple
5	Bearing Specifications	Cylindrical Bearing, id=40mm, length=40mm, wall thickness 10mm, c/r=0.0015, hole dia for oil supply=6mm, 10 holes for pressure data
6	Load Applied	3000N
7	Speed Range	40 to 8000 rpm
8	Permissible Error in Performance	Thermocouple= ± 1°C Pressure= ± 1% Mpa Frictional Torque= ± 2%Nm Shaft Speed= ± 0.1% rpm Flow Rate= ± 0.5%lit/min

`

Table 2: Mechanical Specification

SI NO.	Part detail		Range
1.	Shaft diameter		22 ± 0.005mm
	Journal outer diameter fitted on shaft		40 - 0.005/0.006mm
	Journal inner diameter fitted on shaft		22.035mm
2.	Bearing	Inner dia.	40 + 0.050/006mm
		Width	40.04mm
3.	Radial clearance		0.027mm
4.	Length/ dia. (l/d) ratio		1
	c/r ratio		0.00135
5.	Base plate height from floor		800mm
6.	Journal height from base plate		150mm
7.	Loading bracket height from base plate		760mm
8.	Maximum load		3000N
	Loading ratio		1:5
	Frictional torque distance		51mm
9.	Spindle speed	Min speed	40
		Max speed	8000rpm
10.	Pulley ratio	Speed upto 300 rpm	4:1
		Speed above 300rpm	1:4
11.	Overall size of the machine L*W*H		100*750*1560mm
12.	Weight of the machine		240kg
	Weight of controller		11kg
	Total weight		60kg
13.	Floor size L*W		2000*1500mm
14.	Lubrication unit	Make	Cenlube system
		Oil pressure	5 to 10 bar
		Tank capacity	25 lit
		Size l*b*h	370*290*300mm

`

Table 3: Electrical Specification

S.No.	Part Detail		Range
1	AC Induction motor	Make	Seimens 2.2 kw
		Specifications	2.2 kw, 1435 rpm 415V/ 3 ph/ 50 Hz, 4.4 A, foot mounted
2	Variable frequency drive	Make	TB woods
		Output supply	415V, 5.8 A, 3 ph
		Specifications	2.2 kw, 5.8 A, 415 V, 3 ph
3	AC motor for lubrication	Make; Capacity	SEF Induction motor
		Specifications	0.37 kw, 1350 rpm, 1.2 A, flange mounted, 230 V
		Input supply	230 V/ 50 Hz/ 1 ph, 0.5 A
4	Power Required		2.5 KVA

Table 4: Sensor Specifications

S.No.	Part Detail		Specifications
1	Speed	Sensor	Output from drive
		Range	Min ;40 rpm, Max 8000 rpm
		Least Count	1 rpm
		Accuracy	(1 ± 2% measured speed) rpm
2	Temperature	Type	PT 100, make ; Hot set
		Range	Max 200°C
		Least Count	0.1°C

`

		Accuracy	(0.1 ± 1% measured temp) °C
3	Pressure	Sensor	Digital stainless steel isolated pressure sensor, make ; measurement specialties
		Range	10 Mpa, or 100 bar
		Least Count	0.001 Mpa (1 Kpa)
		Accuracy	(0.001 ± 1% measured value) Mpa
4	Frictional Torque	Sensor	Beam type load cell make ; sensortronics, cap 30 kg
		Range	15 Nm
		Least Count	0.01 Nm
		Accuracy	(0.1 ± 1% measured value) Nm

3.2 SELECTION OF PARAMETERS

As we know that pressure is a function of load mathematically,

$$P = \frac{F}{l.d}$$

Where, P = pressure (Pa)

F = load (N)

l = length of bearing (m)

d = diameter of journal (m)

In my thesis for obtaining the pressure curve of the journal bearing, I considered radial load & journal speed as a influencing factors.

Also, the pressure distribution along with torque and temperature at outlet of the journal bearing has been calculated.

`

For performing the test following parameters are considered as input. There variation are as follows:

Table 5: Input parameters

Experiment No.	1	2
Rotational Speed (rpm)	1800	2400
Load Applied (N)	a) 100	a) 100
	b) 300	b) 300
	c) 500	c) 500

`

Chapter 4

Scope And Objectives

- ✓ To study the basic terminology of 'Tribology'.
- ✓ To analyze the performance of journal bearing under different loading and speed condition.
- ✓ Calculate the design parameters manually for a given experimental setup using mathematical relations and graphs.
- ✓ Solve the Reynolds equation on MATLAB using finite difference method (FDM) and get the value of maximum pressure.
- ✓ Comparing the results which obtained from experimental method with computational method (MATLAB).

`

Chapter 5
Methodology

As we have seen that the tribological study includes friction, lubrication, and wear in their studies, and we also know that, a number of parameters are used to control the journal bearing performance, these are as follows:

i. Load per unit projected area.
ii. Speed in rpm
iii. Lubricant
iv. Dimension such as- diameter of journal (d), clearance between journal bearing (c), length of bearing (l).

But in my thesis I included only first two parameters and rest of the specifications are used as per lab manual instruction. Hence my method of work includes following steps:

- Experiment is being performed on **Journal bearing rig TR-660**, whose experiment setup has explained in chapter 5.
- Calculation of various parameters used in journal bearing performance analysis by manually for a given lubricant SAE 20W40.
- For measuring the property of lubricant performing the test in bio-diesel lab.
- To make a computational model of the journal bearing system MATLAB software is used.
- MATLAB is being used to solve Reynolds equation graphically plotting of pressure drop and number of nodes and then match its results with experimental test on journal bearing.

`

5.1 MATLAB

Mathematical computation using MATLAB

1) MATLAB is being used to generate mathematical results and expected graph of the Experiment.
2) We have consider Reynolds Equation as the driving equation for the lubricating oil film.

$$\frac{\partial}{\partial X}\left(h^3\frac{\partial P}{\partial X}\right)+\frac{X^2}{Z^2}\frac{\partial}{\partial Z}\left(h^3\frac{\partial P}{\partial Z}\right)=\frac{C}{X}\frac{\partial h}{\partial X}$$

3) Applying finite difference method (FDM) for solving this 2-D partial differential equation.
4) The equation which generate after FDM used in MATLAB and get the solution of 2-D Reynolds equation.

`

Chapter 6

Experiment Setting up

6-A Journal bearing test rig TR-660

6.1 Test procedure:

6.1.1 Selection of test bearing

Test bearing is provided is made of leaded bronze material the inner dia. is made with 40.06mm the cylindricity is within 0.003mm and the roundness is within 0.004mm. The l/d ratio of bearing is 1,

6.1.2 Selection of journal

Journal is selected according to the c/r ratio required along with this machine a journal having c/r=0.00135 is supplied.

6.1.3 Preparing machine for testing

- Connect the power input cable to 415v, 50Hz, 3 Phase supply, Switch
- Switch on lubrication motor
- Preparing bearing for test
- Loosen and remove split housing on either ends of self- aligned bearing.
- Insert the bush holder & journal into the shaft ,slide other bush holder
- Place the bearing inside the oil sump at middle ensure the bearing face having sensor p10 is toward front. Insert the bracket over bearing.
- Push shaft with the journal through the bearing and support shaft on the bearing.
- Tighten the lock nut of self-aligned bearing on either end.
- Tighten the pulley on to shaft, loosen motor position align driver pulley in line with driven pulley, pass belt over pulleys and tighten four screw to lock motor position.

`

- Place 1 kg wt. over the loading pan, the bracket is push upward , moves the bearing inside the bracket and position it properly inside bracket , push the journal till it is inside the bearing , lock the journal in place of clamping the bush holder.

6.1.4 Setting pc for test

- Open window 2008 software
- Click on run continuously mode for operating software.
- Click ACQUIRE button to open the acquiring screen
- Enter the file name on remark column
- Enter journal speed and load applied on respective window .
- Click on START button for software to start accepting data initially some values will be displayed on frictional torque these are offset values.
- Click initialize button to bring the pressure valve to zero and zero button for frictional torque to zero.

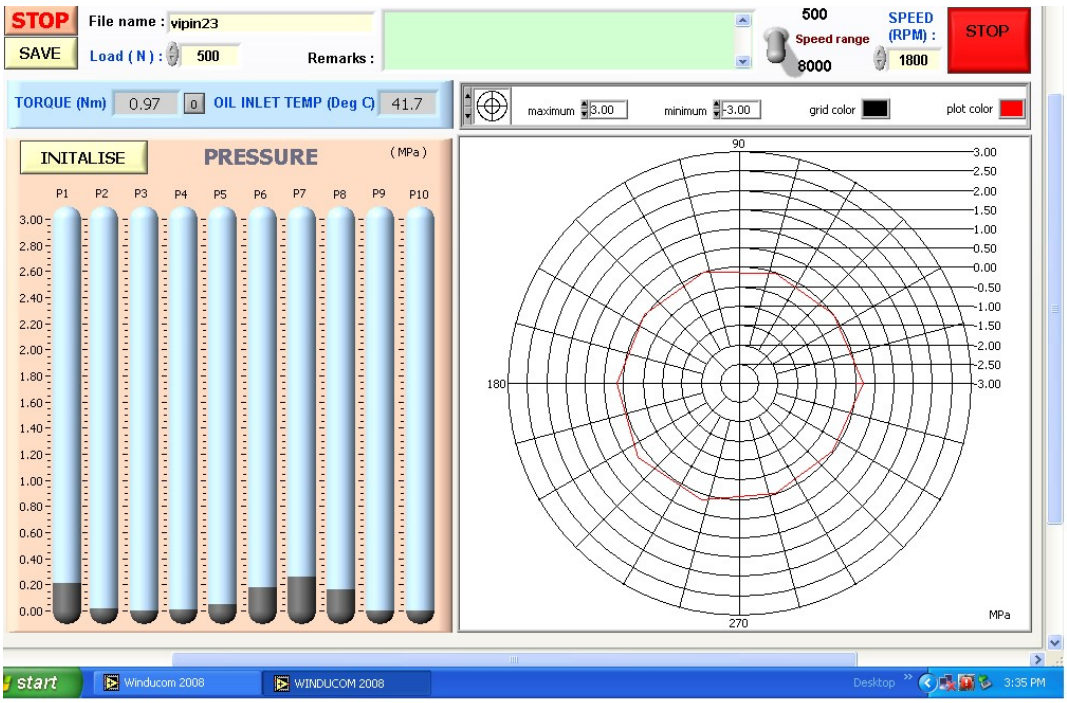

Figure 18: Interface of software used for journal.

`

6.1.5 Test start

- Switch on lube unit and allow oil to run for some time , check oil flow from either ends of bearing equally.
- Set oil pressure looking at gauge on lube unit by turning the pressure valve.
- Set oil discharge by closing or opening the flow control value.
- Ensure oil flows from either ends of bearing.
- Select speed range 40 or 8000 rpm enter the speed required in respectively window, ensure belts is in position 1st if speed required is less than 800rpm, if speed required is above 800rpm the belt is in 2nd position.
- Click RUN MOTOR to start spindle rotation.
- After set aped is reached, place dead weight's on loading pan.
- On pc screen pressure values of different sensor are displayed.
- Wait till the pressure values are steady.

6.1.6 Test end

- Click on MOTOR STOP to end test.

6-B Measuring lubricant properties

6.2 Test Procedure:

6.2.1 Selection of test lubricant

Test lubricant which is used for measuring the property is SAE 20W40. SAE 20W are specified at -18ºC, while SAE 40 are specified at 100ºC. Hence, SAE 20W40 oil must satisfy the 20W viscosity requirement at -18ºC and the 40 requirement at 100ºC.

`

6.2.2 Preparing machine for measuring density

A device which is used for measuring density is “U-Tube Oscillating Apparatus”. Connect power input cable to a device and switch on. This device is used to measure the density at a specified temperature 15ºC. A complete setup for this apparatus is shown below:

Figure 19: A complete setup for U-Tube Oscillating Apparatus.

6.2.3 Test start

Inject the testing oil through a injection to a pipe and keep it for some time till the density reading is displayed, as shown below.

`

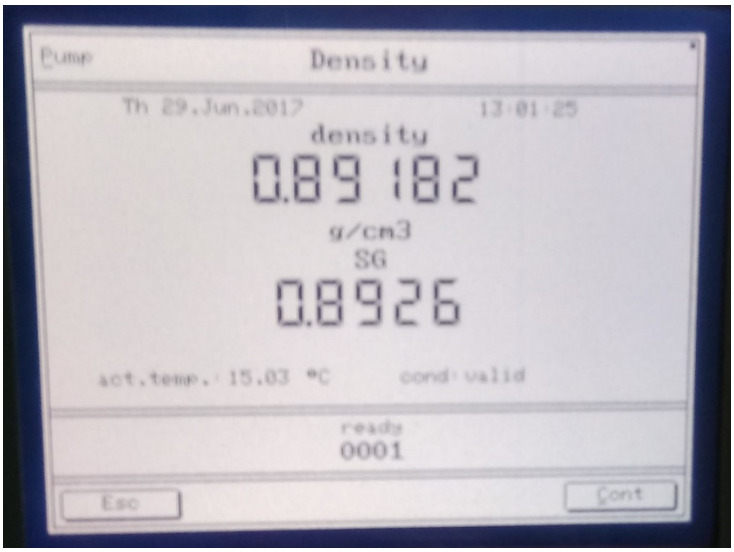

Figure 20: Reading displaying.

6.2.4 For measuring the kinematic viscosity

A device which is used for measuring viscosity is "Automated Kinematic Viscometer." This device is used for measuring kinematic viscosity at temperature 40ºC. Connect power input cable to a device and switch on. A complete setup for this apparatus is shown below:

Figure 21: A complete setup for viscometer.

`

Initially, poured the lubricant oil in the capillary tube up to the marked point as shown in fig 21. After filling the oil, put it in the water bath at the temperature 40ºC as shown in fig.20 and keep it at the same position and start the stopwatch to measure the time till the oil completely reaches to the lower marked point in the capillary tube. Oil depression inside the capillary tube occurs due to the gravity effect.

Figure 22: A schematic diagram for capillary tube.

`

6-C Design procedure of bearing on the basis of mathematical relation

Machine specification has been defined in Table no.2. The parameters which are useful for determining the other bearing parameters, values of these are given below:

- ✓ l/d = 1; c = 0.027mm; c/r = 0.00135; Lubricant = SAE 20W40;
- ✓ Kinematic viscosity, $\nu = 13.5$ mm^2/s; (measured from experiment explain in 6-B)
- ✓ Density (at 15°C), $\rho = 0.8918$ kg/L; (measured from experiment explain in 6-B)
- ✓ Dynamic viscosity, $\mu = 13.64 \times 10^{-3}$ N-s/mm^2;

Steps for bearing design:

Case A: When **rpm = 1800** and **Load applied** = **100N**

Step 1: Unit Bearing Pressure, $P = \frac{F}{l.d} = \frac{100}{20 \times 20} = 0.25$MPa.

Where, F = Radial Load acting on the bearing.
l = Length of bearing.
d = Diameter of journal.

Step 2: Sommerfeld Number, $S = \left(\frac{r}{c}\right)^2 \left(\frac{\mu.n_j}{P}\right) = \frac{(740.74)^2 \times 13.64 \times 10^{-3} \times 30}{0.25 \times 10^6} = 4.490$

Where, S = Sommerfeld Number (Dimensionless).
μ = Dynamic Viscosity of Lubricant (N-s/m^2).
n_j = Journal Speed (rev/s).
p = Unit bearing pressure (MPa).
c = Clearance (mm).

`

After calculating Sommerfeld number it is easy to find the other parameters with the help of charts and table. By using Raimondi and Boyd's charts we get the following values:

Step 3: Eccentricity ratio, ε = 0.021 (from fig. 28)

Step 4: Minimum Film Thickness, $\frac{h_0}{c}$ = 0.97 (from fig. 28)

Step 5: Altitude Angle (Locates the position of minimum film thickness with respect to the direction of the load), ϕ = 84° (from fig. 23).

Step 6: Co-efficient of friction variable, $\left(\frac{r}{c}\right)f$ = 80 (from fig. 24).

Step 7: Flow Variable = $\frac{Q}{r.c.n.l}$ = 3.2 (from fig. 25).

Where, Q = Flow of lubricant drawn into clearance space by journal (mm^3/s).

Step 8: Flow Ratio Variable = $\frac{Q_s}{Q}$ = 0.04 (from fig. 26)

Where, Q_s = Outflow of lubricant from both sides of bearing or side leakage (mm^3/s).

Step 9: Pressure Ratio = $\frac{P}{P_{max.}}$ = 0.55 (from fig. 27)

Where, p_{max} = Maximum pressure developed in lubricant film (MPa or N/mm^2).

`

These results are summaries in the form of table as shown in table 6.

Table 6: Bearing parameters at 1800 rpm

Load (N)	**P (MPa)**	**S**	**E**	$\frac{h_o}{c}$	**Φ**	$\left(\frac{r}{c}\right)f$	$\frac{Q}{rcnl}$	$\frac{Q_s}{Q}$	$\frac{p}{p_{max}}$
100	0.25	4.490	0.021	0.97	84°	80	3.2	0.04	0.55
300	0.75	1.496	0.09	0.91	80°	29	3.3	0.13	0.54
500	1.25	0.898	0.16	0.84	76°	18	3.4	0.21	0.54

Similarly, we can calculate these parameters at 2400 rpm and hence, their results are summaries in table 7.

Table 7: Bearing parameters at 2400 rpm

Load (N)	**P (MPa)**	**S**	**E**	$\frac{h_o}{c}$	**Φ**	$\left(\frac{r}{c}\right)f$	$\frac{Q}{rcnl}$	$\frac{Q_s}{Q}$	$\frac{p}{p_{max}}$
100	0.25	5.987	0.019	0.98	84°	110	3.2	0.02	0.55
300	0.75	1.995	0.07	0.93	81°	39	3.2	0.09	0.54
500	1.25	1.196	0.12	0.88	78°	23	3.3	0.16	0.54

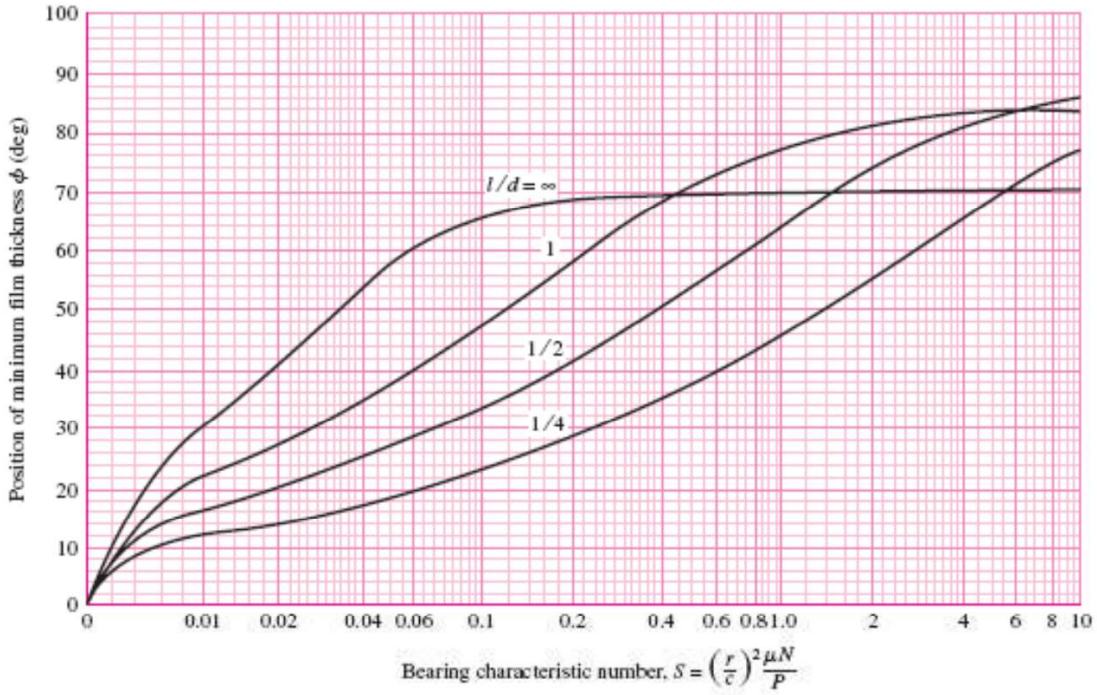

Figure 23: **Position of Minimum Film Thickness vs. Bearing Characteristic Number.**

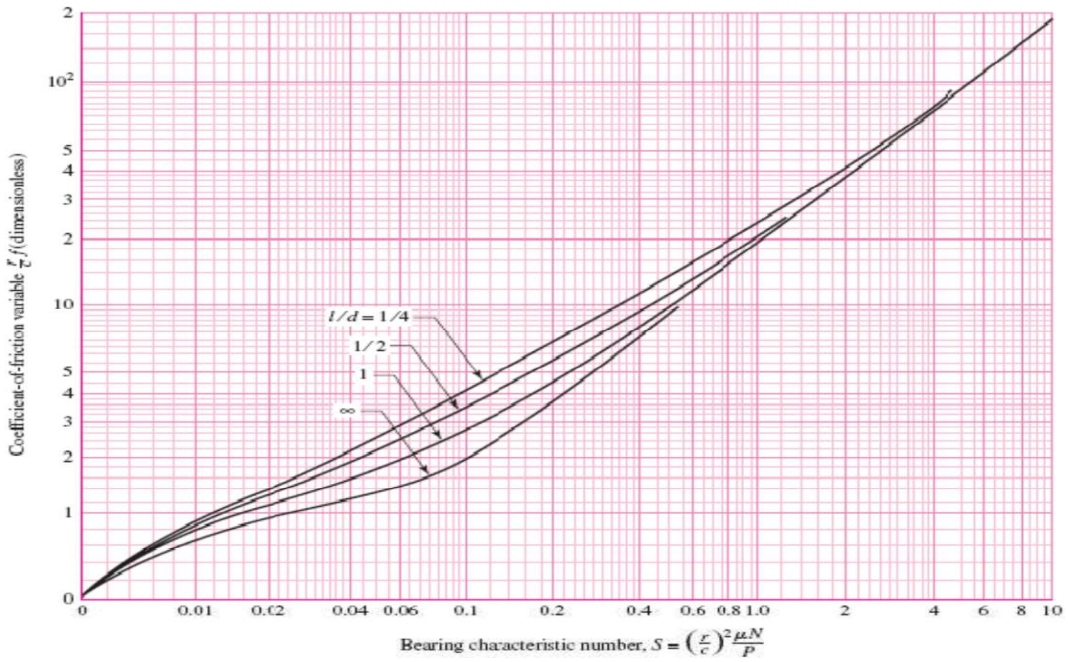

Figure 24: Coefficient of friction variable vs. Bearing Characteristic Number.

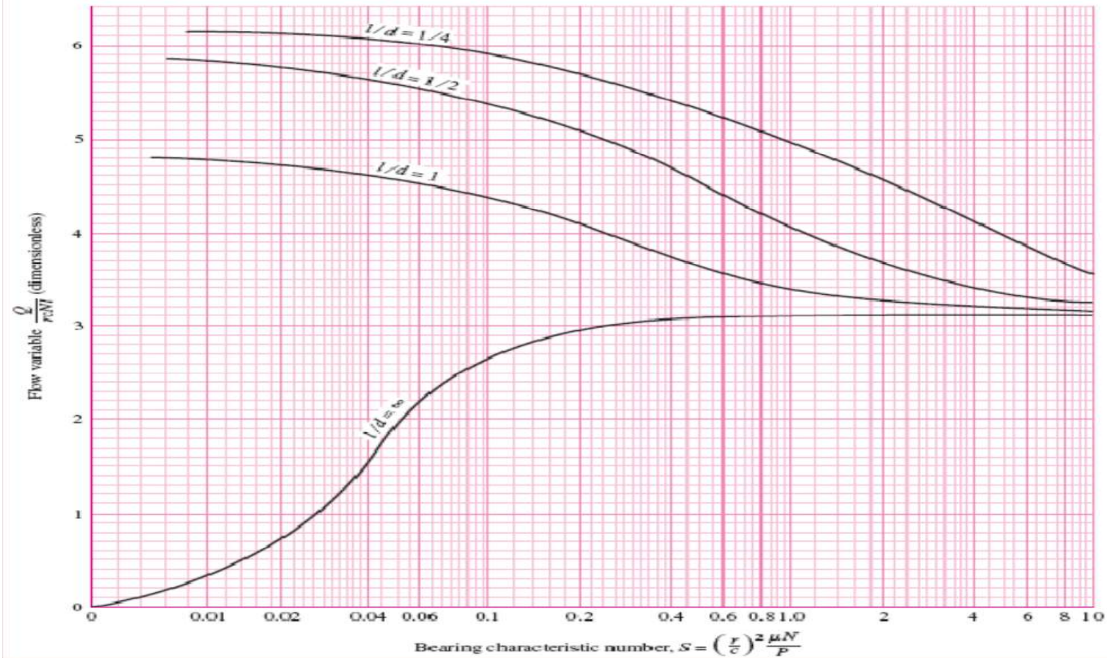

Figure 25: Flow Variable vs. Bearing Characteristic Number.

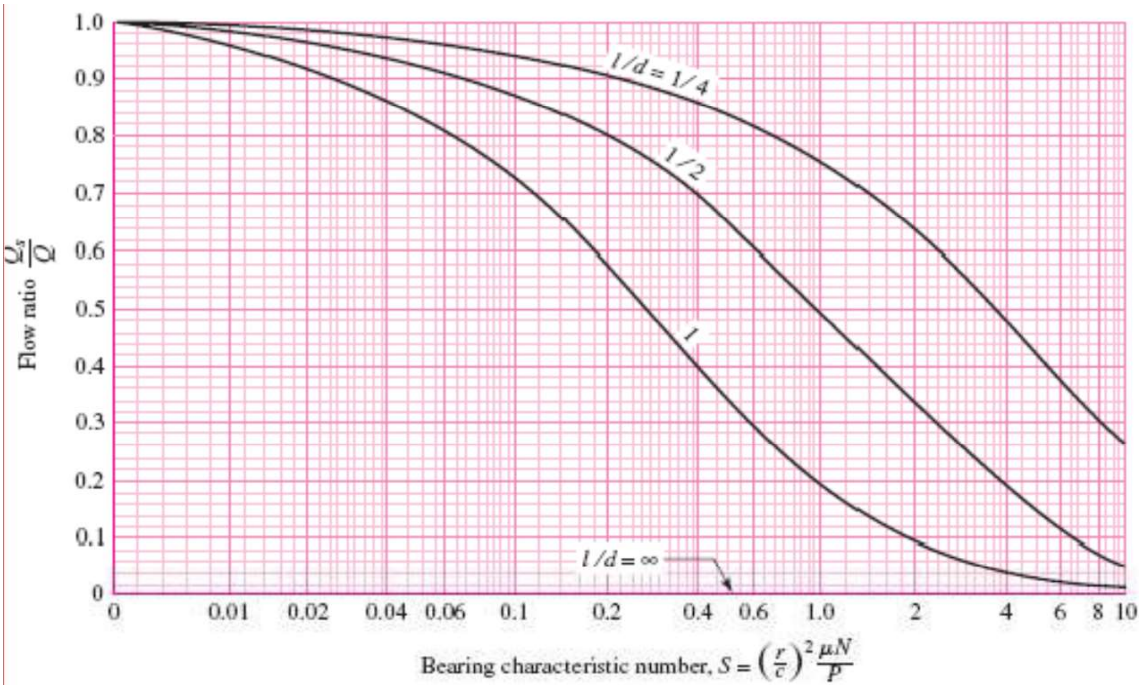

Figure 26: Flow Ratio vs. Bearing Characteristic Number

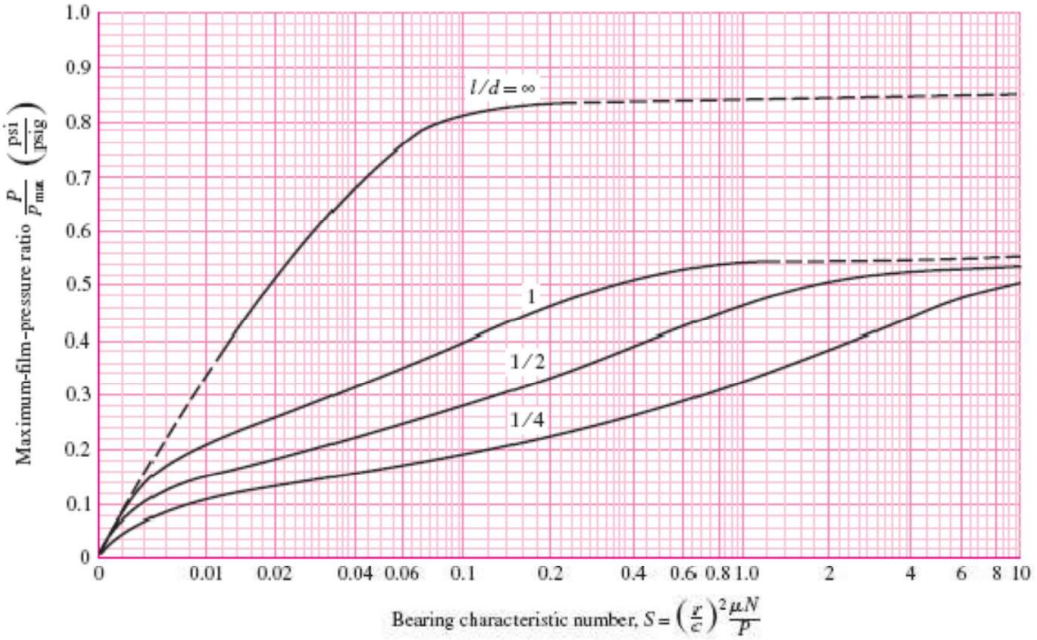

Figure 27: Minimum Film pressure ratio vs. Bearing Characteristic Number.

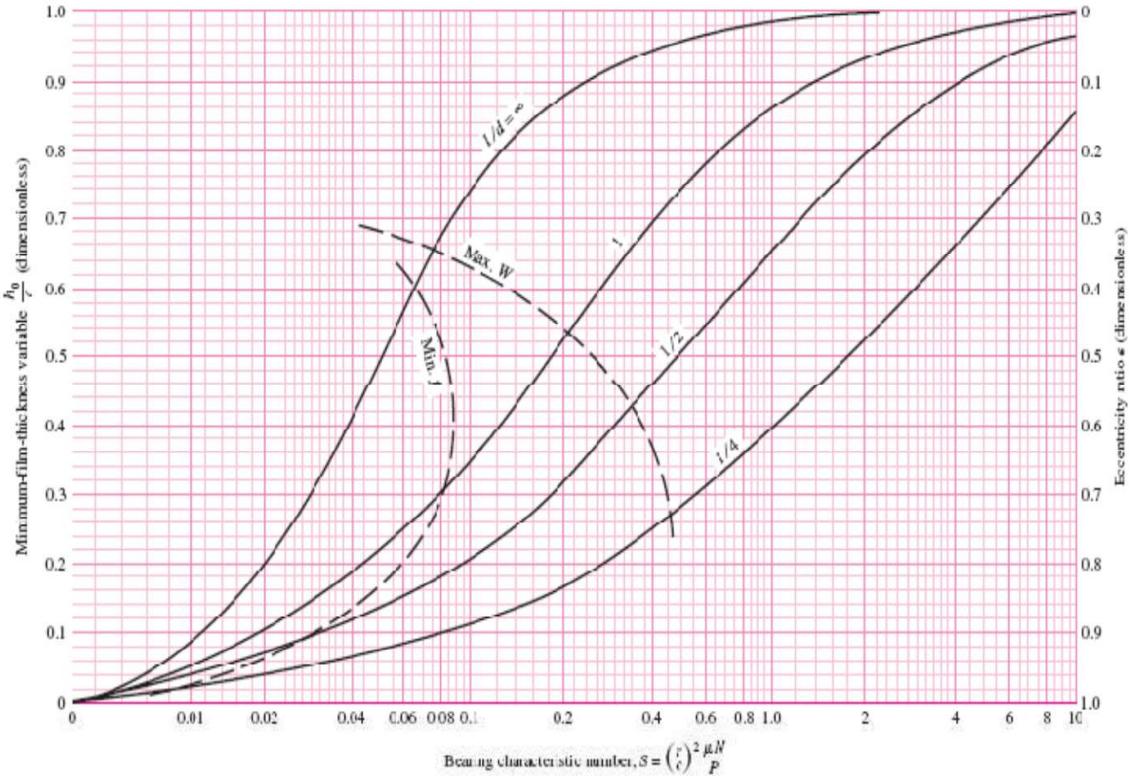

Figure 28: Minimum film thickness variable vs. Bearing Characteristic Number.

`

Chapter 7

Results and Conclusion

7.1 Experimental Results:

Graphs at constant speed 1800 rpm and variable load.

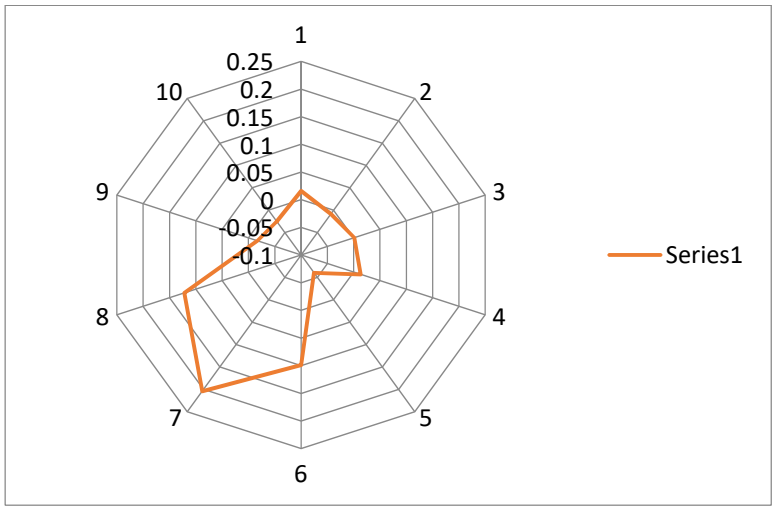

Figure 29 : Pressure variation at 100 N load.

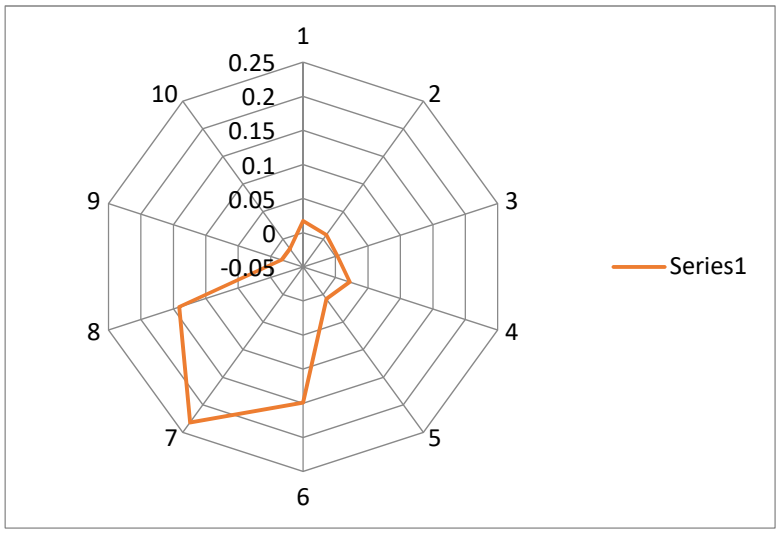

Figure 30: Pressure variation at 300N load.

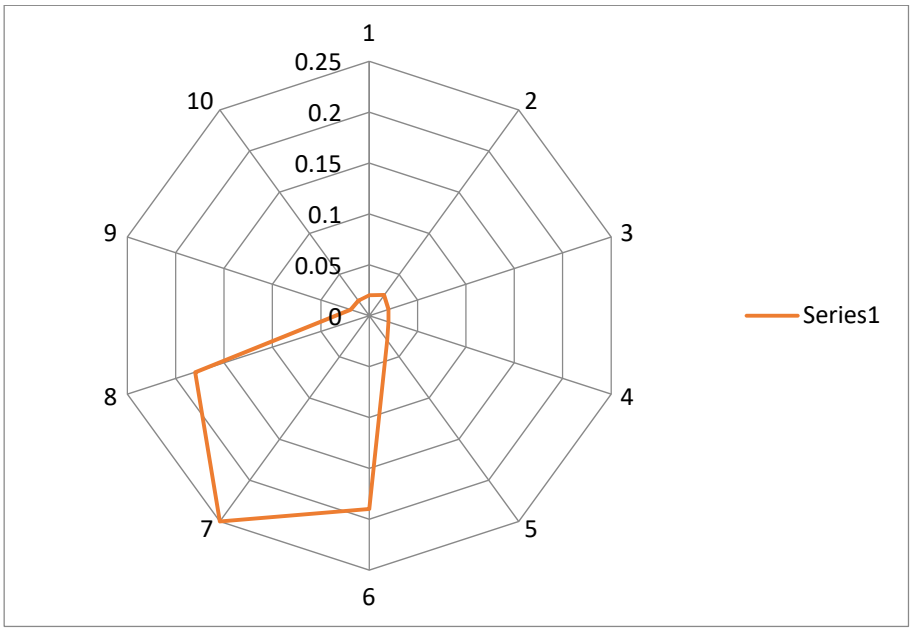

Figure 31: Pressure variation at 500N load.

Combined Effect on Pressure distribution at 1800 rpm.

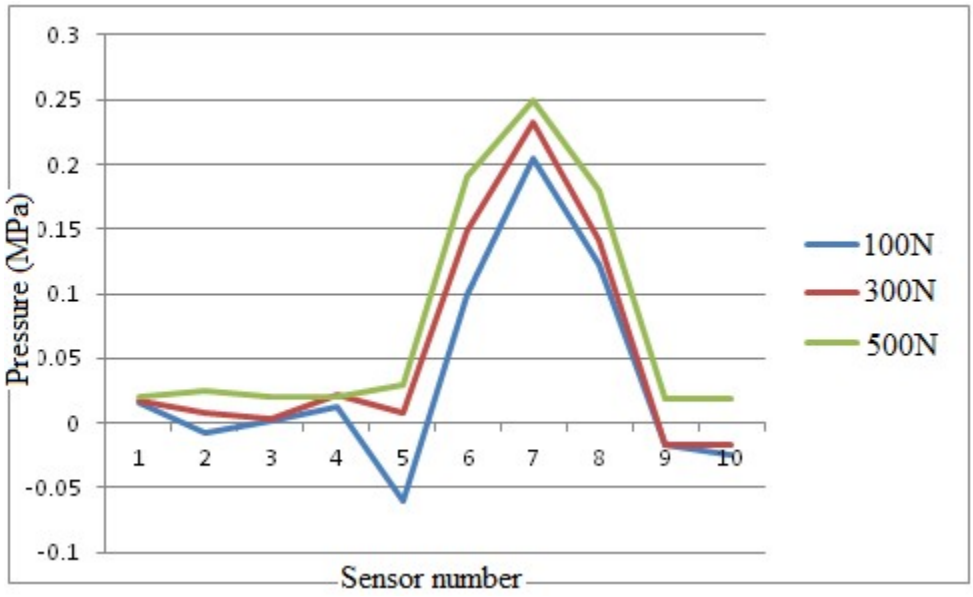

Figure 32: Pressure variation at 100N,300N,500N load respectively.

`

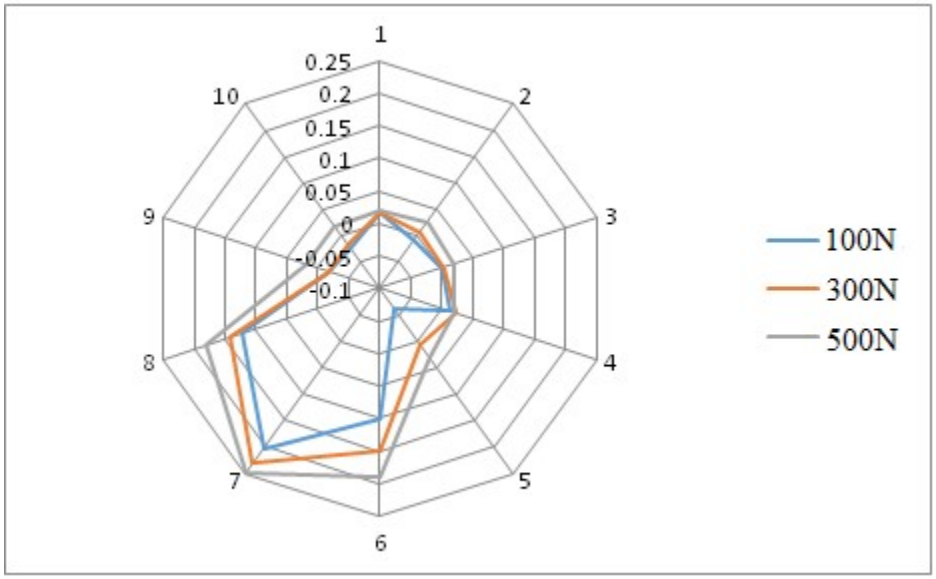

Figure 33: Comparison of pressure distribution at different load.

Graphs at constant speed 2400 rpm and variable load.

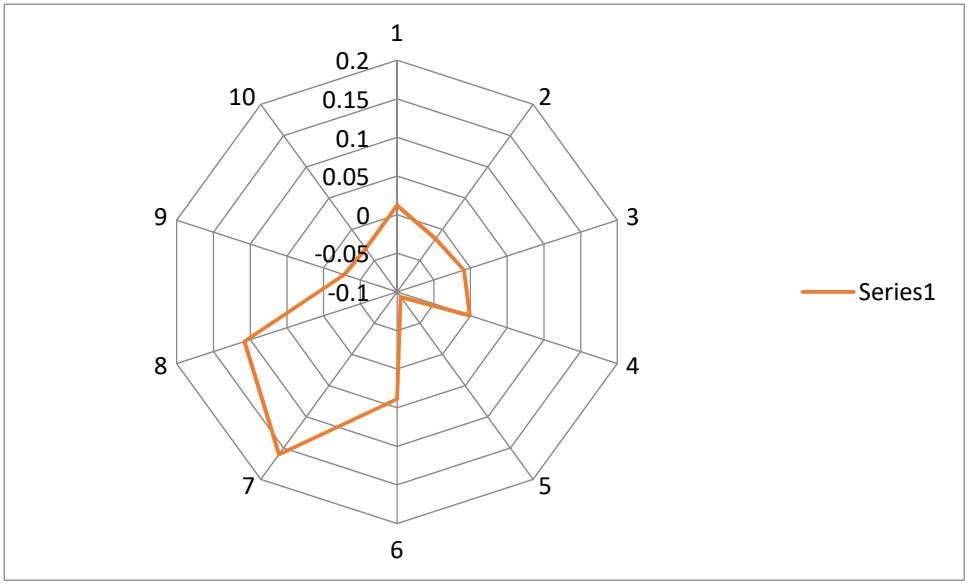

Figure 34: Pressure variation at 100N load and 2400rpm.

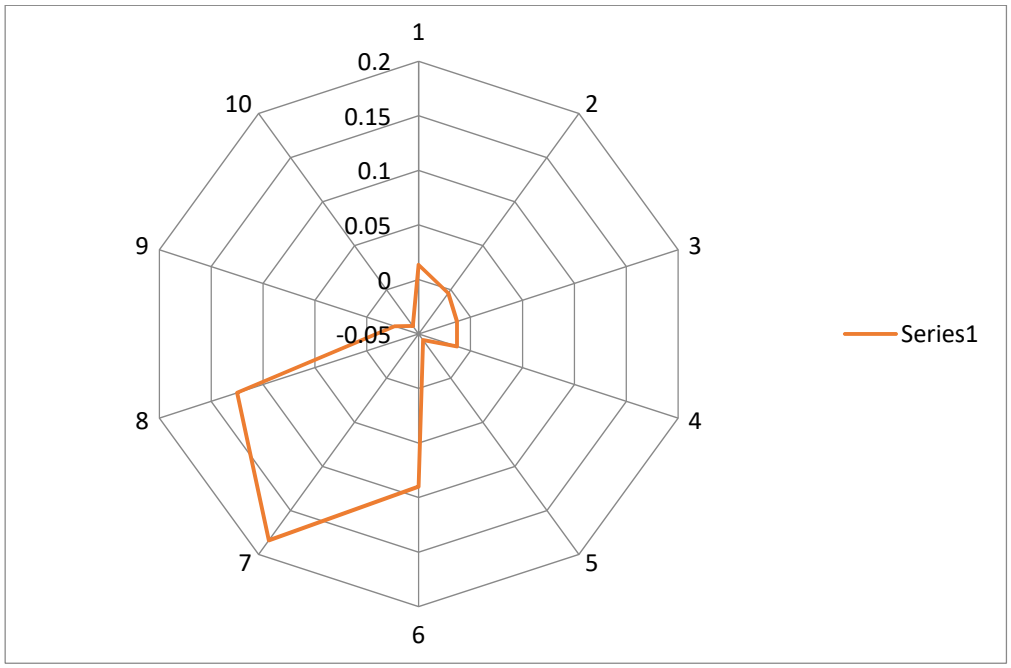

Figure 35: Pressure variation at 300N load and 2400 rpm.

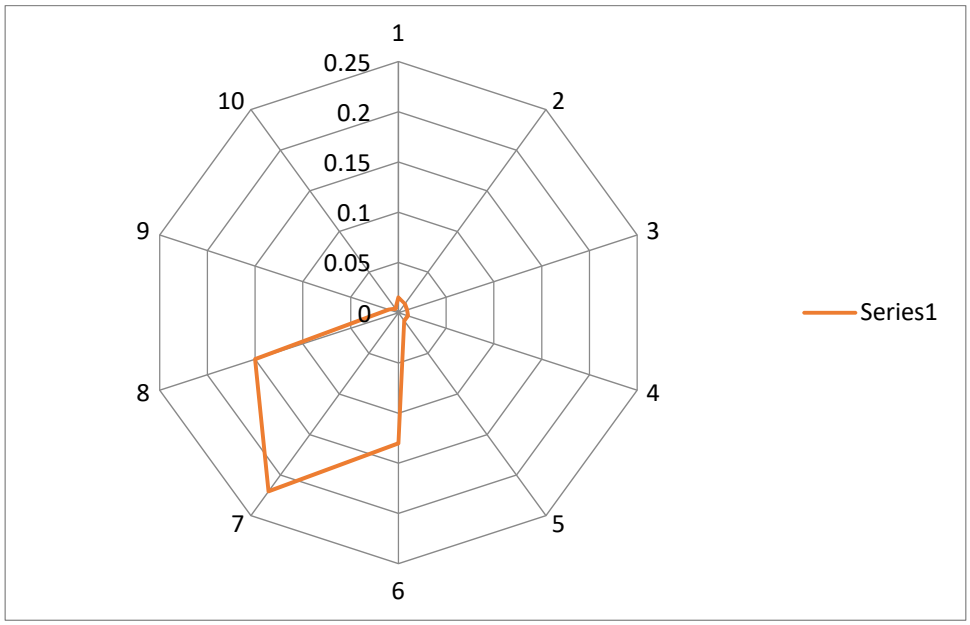

Figure 36: Pressure variation at 500N load and 2400 rpm.

`

Combines effect on Pressure Disribution at 2400 rpm.

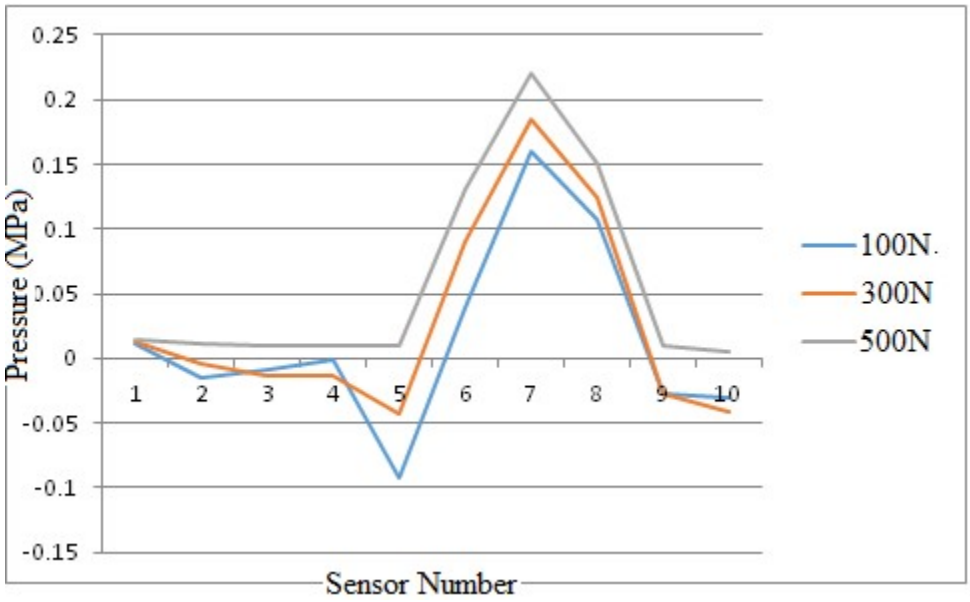

Figure 37: Pressure variation at 100N,300N,500N load respectively.

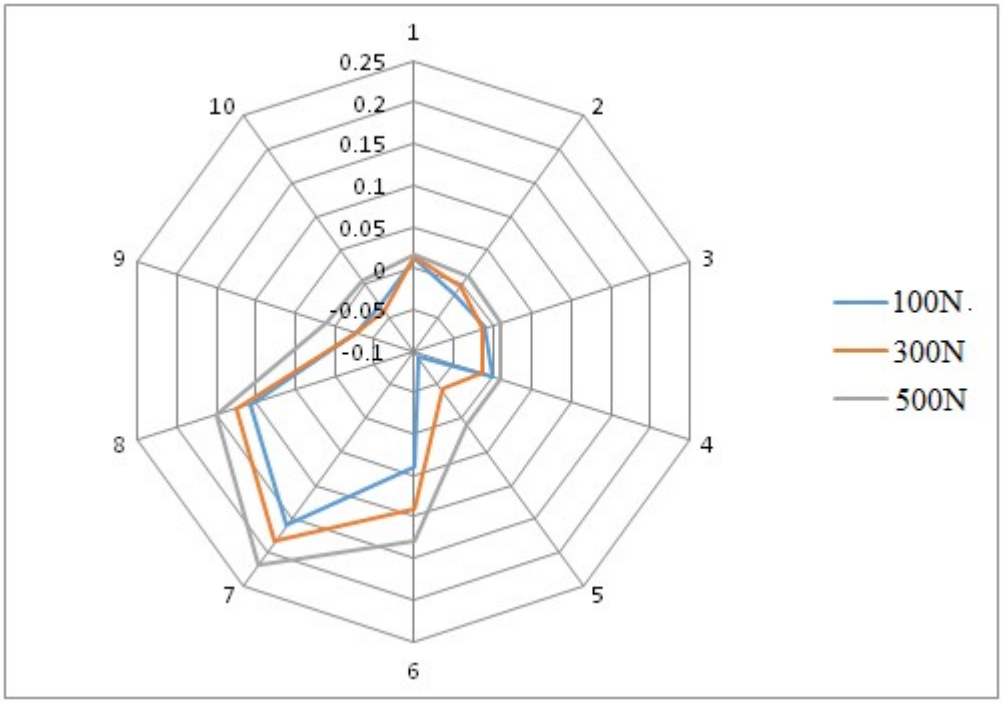

Figure 38: Comparison of pressure distribution at different load.

`

Graphs at different speed but constant load 100N

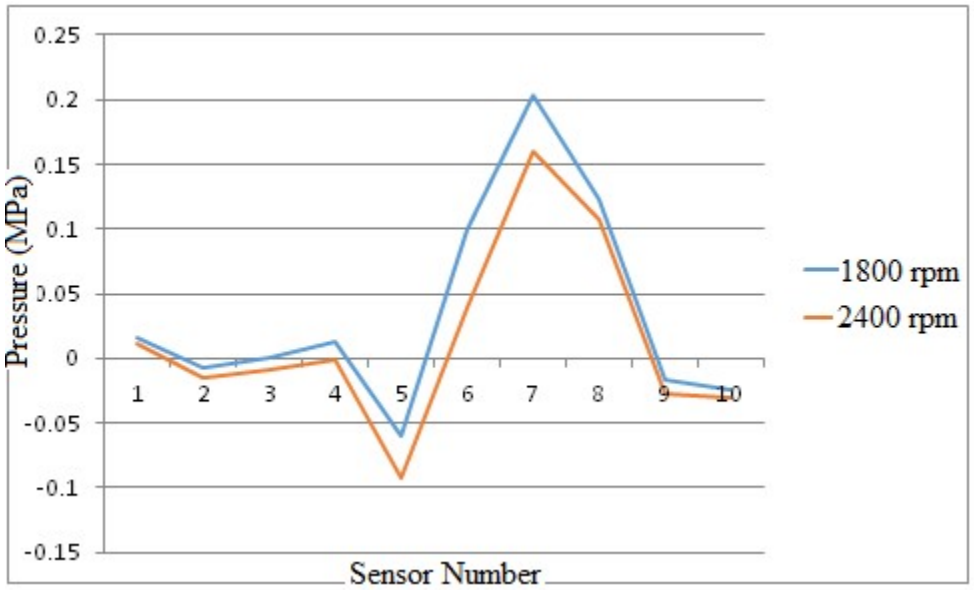

Figure 39: Pressure variation at 1800 rpm and 2400 rpm

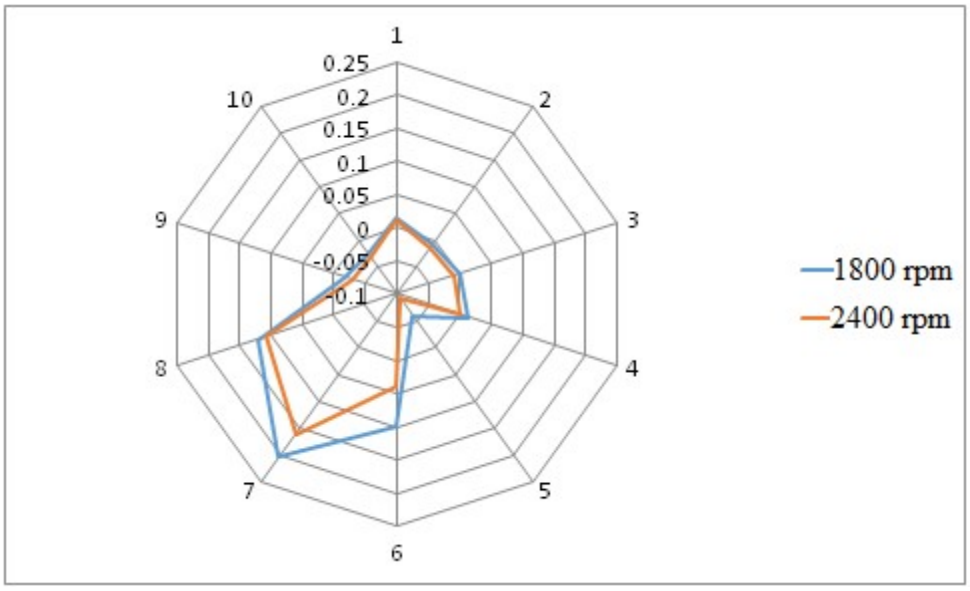

Figure 40: Comparison of pressure at different speed.

`

It can be seen from figure (22-29) that the pressure distribution curve formed from the concordant reading shows maximum value around 7^{th} sensor.

It is also observed that with the increase in load the maximum pressure value increases as shown in figure (25 & 30).

Further, from figure (32 & 33) it is observed that with the increase in speed the pressure increases but further more increase in speed it decreases.

7.2 MATLAB results

The governing 2-D Reynolds differential equation which is solved in appendix, the analytical solutions are not possible for finite length journal bearing hence, numerical methods are used. Therefore, a numerical solution of 2-D Reynolds equation for a finite journal bearing (describe in chapter 5 in article 5.1) solved in MATLAB. The result of MATLAB, are shown in figure (34).

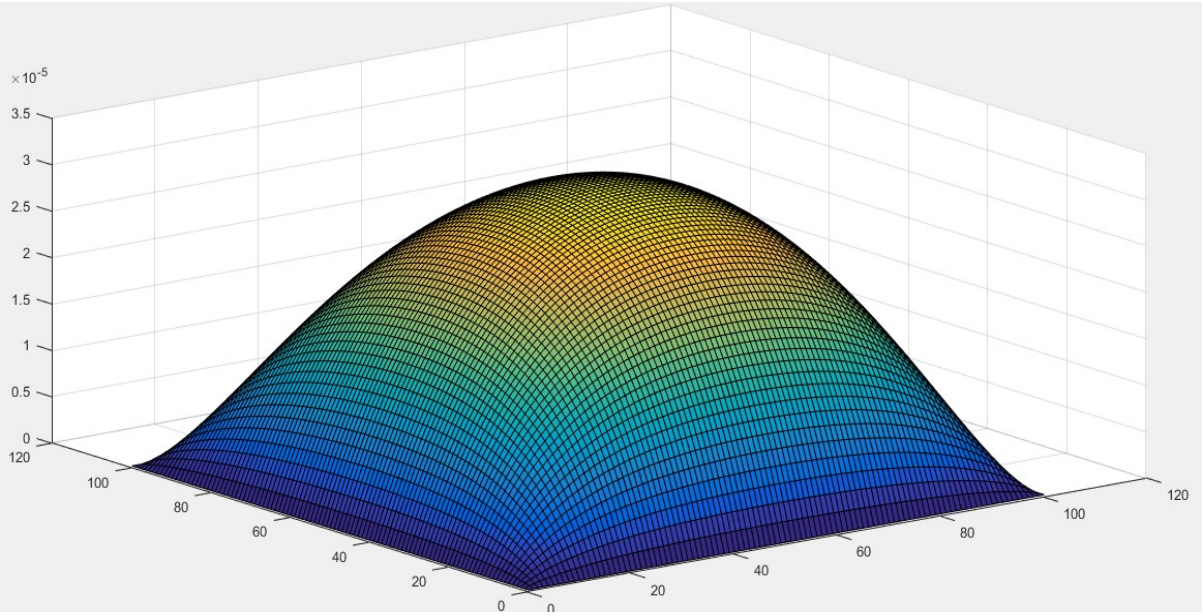

Figure 41: Pressure distribution at the circumference of journal.

`

Thus the pressure at any mesh point (i, j) is expressed in terms of pressure at four adjacent points. The accuracy of result depends upon number of iteration used.

7.3 Conclusion

- It is observed from the experiment performed on Journal bearing test rig TR-660, the variation in load and speed effect the pressure distribution as shown in figure (22-33).
- It is also observed that as load increases the value of maximum pressure increases for a given rotational speed (25 & 30).
- It is also observed that with increase in journal speed, the pressure increases but more increase in speed shows the negative effect on pressure.
- The accuracy of pressure distribution curve which is obtained from MATLAB depends upon nodes points and number of iteration which is used.

`

Chapter 8
Future Scope

In my thesis work I have include only pressure distribution and load effect on journal bearing but apart from this, the oil film thickness and oil temperature are also effects the journal bearing performance. Hence, from the future respect point, the themal analysis can be done and behavior of journal bearing can observe under this consideration.

As I have discussed about Tribology (in article 1.1) the lubrication oil also effect the journal bearing performance. Hence, by using different types of lubricating oil its performance can be determined from future prospect.

Nowadays tribology is a wide-ranging multi-disciplinary field of study and research investigating the lifecycle, durability, reliability and efficiency, of every manufactured mechanical system around the globe.

From future point of view we can calculate the wear and coefficient of friction, by conducting experiment on pin on disc test rig, through which we are able to determine the service life of a component which are in relative motion. As we know at present, global warming is a severe challenge as more than 75% of energy is produced from fossil fuels. Hence, to solve the problem related to global warming and finite fossil fuel supplies we have to solve the problems of energy shortage, excessive consumption and greenhouse gas emission. Hence, improving the energy efficiency of resource use and reducing the emission of greenhouse gases are now very important issues in the world, especially for transportation and industry. So for this purpose from future respect point we can study about the green tribology. Here, the brief discussion about green tribology is given below:

Green tribology, dealing with the preservation of energy, environmental protection as well as improving quality of life and tells about lifecycle, durability, reliability and efficiency, of every manufactured mechanical system around the globe.

`

REFERENCES

1. Alexey Kornaev, Leonid Savin, Elena Kornaeva, Alex Fetisov: “Influence of the ultrafine oil additives on friction and vibration in journal bearings,” Vol. 101, pp.131-140, 2016.
2. Feng Cheng, Wei xi Ji: “A velocity-slip model for analysis of the fluid film in the cavitation region of a journal bearing,” Vol. 97, pp.163-172, 2016.
3. S. Baskar, G. Sriram & S. Arumugam: “Tribological Analysis of a Hydrodynamic Journal Bearing Under the Influence of Synthetic and Biolubricants,” http://dx.doi.org/10.1080/10402004.2016.1176285, 2016.
4. Zissimos, P. Mourelatos: “An Efficient Journal Bearing Lubrication Analysis For Engine Crankshafts,” Tribology Transcations., 44 (3), pp. 351-358, 2001.
5. Erol Feyzullahoglu, Nehir Sakiroglu: “The wear of aluminum-based journal bearing materials under lubrication, Materials and Design,” Vol. 31, No. 5, pp. 2532-2539, 2010.
6. Massimo Del Din, Elisabet Kassfeldt: “Wear characteristics with mixed lubrication conditions in a full scale journal bearing,” Wear, Vol. 232, No. 2, pp. 192-198, 1999.
7. Sun, J., and Gui, C. L.: “Hydrodynamic Lubrication Analysis of Journal Bearing Considering Misalignment Caused by Shaft Deformation,” Tribol. Int. 37, pp. 841–848, 2004.
8. Qian (Jane) Wang, Fanghui Shi and Si C. Lee: “A Mixed-Lubrication Study of Journal Bearing Conformal Contacts,” J.Tribol 119/(3), 456-461, 1997.
9. McKee, S. A., and McKee, T. R.: “Pressure Distribution in Oil Film of Journal Bearings,” ASME, RP-54-8, 5, pp. 149–165, 1932.
10. Booker, J. F., and Huebner, K. H.: "Application of Finite Element Methods to Lubrication: An Engineering Approach," ASME JOURNAL OF LUBRICATION TECHNOLOQY, Oct., pp. 313-323, 1972.

`

11. Bush, A. W., Gibson, R. F., and Thomas, T. R.: "The Elastic Contact of a Rough Surface," Wear, Vol. 35, pp. 87-111, 1975.
12. Dubois, G., Ocvirk, F., and Wehe, R.: “Experimental Investigation of Misaligned Couples and Eccentricity at Ends of Misaligned Plain Bearings,” NACA, TN 3352, 1955.
13. Mokhtar, M. O., Safar, Z. S., and Abd-El-Rahman, M. A.: “An Adiabatic Solution of Misaligned Journal Bearings,” ASME J. Tribol.107 , pp. 263–267, 1985.
14. Buckholz, R. H., and Lin, J. F.: “The Effect of Journal Bearing Misalignment on Load and Cavitation for non-Newtonian Lubricants,” ASME J. Tribol., 108, pp. 645–654, 1986.
15. Vijayaraghavan, D., and Keith, T. G.: “Effect of Cavitation on the Performance of a Grooved Misaligned Journal Bearing,” Wear [CrossRef], 134, pp. 377–397, 1989.
16. Rao T.V.V.L.N., Rani A.M.A., Nagarajan T., and Hashim F.M.,: “Analysis of slider and journal bearing using partially textured slip surface,” Tribology International, 56, (2012), 121–128.
17. Kai Feng, Xueyuan Zhao, Caijiao Huo and Zhiming Zhang: “Analysis of novel hybrid bump-metal mesh foil bearings,” Tribology International., 103, pp.529–539, 2016.
18. San Andrés L and Chirathadam TA. “A metal mesh foil bearing and a bump-type foil bearing: comparison of performance for two similar size gas bearings,” J Eng Gas Turbines Power 2012;134:102501.
19. Nacer Tala-Ighil and Michel Fillon: “A numerical investigation of both thermal and texturing surface effects on the journal bearings static characteristics,” Tribology International, Vol. 90, pp. 228-239, 2015.
20. Mufti RA, Priest M.: “Theoretical and experimental evaluation of engine bearing performance,” Proc Inst Mech. Eng. Part J:J Eng Tribol. Vol. 223, pp. 629–44, 2009.
21. Khonsari MM, Booser ER.: "Applied tribology: bearing design and lubrication,” INC: John Wiley and Sons; 2001.

`

22. Buscaglia GC, Ciuperca I and Jai M.: "The effect of periodic textures on the static characteristics of thrust bearings," J. Tribol. Vol. 127, pp. 899–902, 2005.
23. Fowel M, Olver AV, Gosman AD, Spikes HA and Pegg I.: "Entrainment and inlet suction: two mechanisms of hydrodynamic lubrication in textured bearings," J. Tribol.; Vol. 129, pp. 336–47, 2007.
24. Tala-Ighil N, Fillon M and Maspeyrot P.: "Effect of textured area on the performances of a hydrodynamic journal bearing," Tribol. Int. Vol. 44(3), pp. 211–219, 2011.
25. Reynolds O.: "On the theory of lubrication and its application of Mr.Beauchamp Tower's Experiments," Philos Trans R Soci. Vol.177(1), pp. 157–234, 1886.
26. Tala-ighil N, Bounif A, Maspeyrot P.: "Thermo-hydrodynamic study of the journal bearing under static load," Proc Inst Mech. Eng. Part C: J Mech. Eng. Sci Vol. 222(9), pp. 1801–1809, 2008.
27. Kun Li, Jie Liu, Xu Han, Chao Jiang, Hongjun Qin: "Identification of oil-film coefficients for a rotor-journal bearing system based on equivalent load reconstruction," Tribo. Int. Vol. 104, pp. 285–293, 2016.
28. Tiwari R, Lees AW, Friswell MI, "Identification of dynamic bearing parameters: a review," Shock Vib. Dig. Vol. 36(2), pp. 99–124, 2006 http://dx.doi.org/10.1177/ 0583102404040173.
29. Tønder K., "Dimpled pivoted plane bearings: Modified coefficients," Tribol Int 2010; 43(2010): 2303–7. http://dx.doi.org/10.1016/j.triboint.2010.08.001.
30. Tieu AK, Qiu ZL., "Identification of sixteen dynamic coefficients of two journal bearings from experimental unbalance responses," Wear 1994; 177:63–9. http://dx.doi.org/10.1016/0043-1648(94)90118-X.
31. Qiu ZL, Tieu AK., "Identification of sixteen force coefficients of two journal bearings from impulse responses," Wear 1997; 212:206–12. http://dx.doi.org/ 10.1016/S0043-1648(97)00154-3.
32. Jiang GD, Hu H, Xu W, Jin ZW, Xie YB, "Identification of oil film coefficients of large journal bearings on a full scale journal bearing test rig," Tribol Int 1997; 30 (11):789–93. http://dx.doi.org/10.1016/S0301-679X(97)00040-6.

`

33. Ma Chenbo, Zhu Hua, An optimum design model for textured surface with elliptical-shape dimples under hydrodynamic lubrication, Tribology International, 44, (2011), 987–995.
34. Tala-Ighil Nacer, Fillon Michel, A numerical investigation of both thermal and texturing surface effects on the journal bearings static characteristics, Tribology International, 90, (2015), 228–239.
35. Meng, F. M., Zhang L., Li T.T., Thermal analysis of micro textured journal bearing using non-Newtonian rheology of lubricant and JFO boundary conditions using FSI, Tribology International, 69, (2014), 19–29.
36. Md. Ali Ahmad and Gupta K.C., Effect of oil groove location on the temperature and pressure in hydrodynamic journal bearings, Tribology International, 42, (2009), 487–492.
37. F.P. Brito and Chan L., Assessment of journal bearing with either one or two axial grooves located to the load line to improve its performance, Tribology International, 40, (2007), 929–936.
38. Christensen, H., and Tonder, K., "The hydrodynamic lubrication of rough journal bearing", SINTEF research report No.72/166-172, 1971.
39. Wang, Q., Shi, F., and Lee, S.C., "A mixed-lubrication study of journal bearing conformal contacts", ASME/STLE joint tribology conference/456-61, 1997.
40. Vijayaraghavan, D., and Brewe, D.E., "Effect of rate of viscosity variation on the performance of journal bearings", Journal of tribology/1-7, 1998.
41. Poddar, S., and Tandon, N., "Detection of journal bearing vapour cavitation using vibration and acoustic emission techniques with the aid of oil film photography", Tribology International/1-21, 2016.
42. Santos, E.N., Blanco, C.J.C., Macedo, E.N., Maneschy, C.E.A., Quaresma, J.N.N., "Integral transform solutions for the analysis of hydrodynamic lubrication of journal bearings", Tribology international/161-169, 2012.

`

43. Harnoy, A.., "Model-based investigation of friction during start-up of hydrodynamic journal bearings", Journal of tribology/667-73, 1995.
44. Christensen, H., and Tonder, K., "The hydrodynamic lubrication of rough journal bearing", SINTEF research report No.72/166-172, 1971.
45. Tzeng, S.T., and Saibel, E., "On the effects of surface roughness in the hydrodynamic lubrication theory of a short journal bearing", wear/179-84, 1967.
46. Gengyuan, G., Yin, Z., Jiang, D., and Zhang, X., "Numerical analysis of plain journal bearing under hydrodynamic lubrication by water", Tribology International/31-38, 2014.
47. Tsai, H.J., and Jeng, Y.R., "Characteristics of powder lubricated finite width journal bearings: A Hydrodynamic analysis", ASME, Journal of tribology/351-57, 2006.
48. Soto, L.U., Santoscoy, R.S., Parra, M.P., Relvich, A.C.R., and Valdez R.Y., "Rotor dynamic optimization of fixed pad journal bearings using response surface design of experiments", Journal of Engineering for gas turbines and power/1-10, 2016.
49. T.A.Stolarski, R.Gawarkiewicz, K.Tesch: "Acoustic journal bearing-A search for adequate configuration," Tribol Int. Vol. 92, pp. 387-394, 2015.
50. Wiesendanger M. "Squeeze film air bearing using piezoelectric bending elements," Ph.D. thesis. Switzerland: Ecole Polytechnique Federalede Lausanne; 2001.
51. Yoshimoto S, Anno Y, Hamanaka K. "Float characteristics of squeeze-film gas bearing with elastic hinges for linear motion guide," JSME Int. J. 1997;40:353.
52. Azzedine Dadouche, Martin J. Conlon, "Operational performance of textured journal bearings lubricated with a contaminated fluid," Tribol Int. Vol. 93, pp. 377-389, 2016.

53. Duchowski J, Collins KG, Dmochowski W, “Experimental evaluation of filtration requirements for journal bearings operating under different contaminant levels,” Lubr. Eng. 2002; 6: 34–9.
54. Dadouche A, Conlon MJ, Dmochowski WM, Koszela W, Galda L, Pawlus P, “Experimental evaluation of steady-state and dynamic performance of hydro-dynamic journal bearings: plain versus textured-surface,” In: Proceedings of the 10th EDF/P prime workshop, Futuroscope, France; Oct.6–7, 2011.
55. Dadouche A, Conlon MJ., “Reflections on journal bearings performance with surface texturing,” In: Proceedings of the 5th world Tribology congress, Torino, Italy; Sep.8–13, 2013.
56. Dadouche A, Conlon MJ, Dmochowski WM, Koszela W, Galda L, Pawlus P, “Effect of surface texturing on the steady-state properties and dynamic coef-ficients of a plain journal bearing: experimental study,” In: Proceedings of ASME Turbo Expo 2011, Vancouver, BC, Canada; June6–10, 2011.
57. Iwamoto K, Tanaka K, “Influence of manufacturing error for characteristics of cylindrical journal bearing,” In: Proceedings of the 31th leeds-lyon symposium on tribology, Leeds, UK; Sept.7–10, 2004.
58. Tianming Ren, Ming Feng, “Stability analysis of water-lubricated journal bearings for fuel cell vehicle air compressor,” Tribol Int. Vol. 95, pp. 342-348, 2016.
59. Walton James F, Tomaszewski Michael J, Heshmat H, “The role of high perfor-mance foil bearings in advanced, oil-free, high-speed motor driven compressors,” In: Proceedings of the 1st international conference on fuel cell science, engineering and technology. Rochester, NewYork, USA: ASME; 2003.P. 411–17.
60. Swanson EE, Heshmat H, Shin JS, “The role of high performance foil bearings in an advanced, oil-free, integral permanent magnet motor driven, high-speed turbo-compressor operating above the first bending critical speed[C],” In: Proceedings of the ASME Turbo Expo. Amsterdam, The Netherlands; 2002. p. 1119–125.
61. Hashimoto H, Wada S, Ito J, “An application of short bearing theory to dynamic characteristics problems of turbulent journal bearings,” J Tribol 1987;109:307–14.

62. Norifumi Miyanaga, Jun Tomioka, “Effect of support stiffness and damping on stability characteristics of herringbone-grooved aerodynamic journal bearings mounted on viscoelastic supports,” Tribol Int. Vol.100, pp. 195-203, 2016.
63. Vohr JH, Chow CY, “Characteristics of herringbone-grooved, gas-lubricated journal bearings,” Trans ASME J Basic Eng 1965; 87(3): 568–78. http://dx.doi. org/10.1115/1.3650607.
64. Chow CY, Vohr JH, “Helical-grooved journal bearing operated inturbulent regime,” Trans ASME J Lubr Technol 1970; 92(2): 346–57. http://dx.doi.org/ 10.1115/1.3451407.
65. Kawabata N, Ozawa Y, Kamiya S, Miyake Y, “Static characteristics of the regular and reversible rotation type herringbone grooved journal bearing,” Trans ASME J Tribol 1989; 111(3): 484–90. http://dx.doi.org/10.1115/1.3261955.
66. Tiago H. Machado, Katia L. Cavalca, “Investigation on an experimental approach to evaluate a wear model for hydrodynamic cylindrical bearings,” Applied Mathematical Modelling, Vol. 40, pp. 9546-9564, 2016.
67. B. Lüneburg, D. Dettmar, M. Medhioub, D. Thomas, U. Mermertas, H. Schwarze, E. Schüler, S. Kühl, E.G. Welp, “Advancement of a radial journal bearing for highest load capacity of big steam turbines for power generation,” in: Proceedings of Seventh International Conference on Rotordynamics, IFToMM 2006, vol. 1, TU Vienna, Vienna, 2006, pp. 1–10 .
68. M. Mokhtar, R. Howarth, P. Davies, “Wear characteristics of plain hydrodynamic journal bearings during repeated starting and stopping,” ASLE Trans. 20 (1977) pp. 191–194.
69. J.M. Bouyer, M. Fillon, I. Pierre-Danos, “Influence of wear on the behavior of a two-lobe hydrodynamic journal bearing subjected to numerous startups and stops,” J. Tribol. 129, pp. 205–208, 2007.
70. P.G. Nikolakopoulos, C.A. Papadopoulos, “A study of friction in worn misaligned journal bearings under severe hydrodynamic lubrication,” Tribol. Int. Vol. 41, pp.461–472, 2008.

`

71. T.H. Machado, K.L. Cavalca, “Geometric discontinuities identification in hydrodynamic bearings,” In: Proceedings of Ninth International Conference on Rotor Dynamics, IFToMM-2014, 1, Politecnico di Milano, Milan, Italy, pp. 1–10, 2014.
72. M. Arghir, A. Alsayed, D. Nicolas, “The finite volume solution of the Reynolds equation of lubrication with film discontinuities,” Int. J. Mech. Sci. 44, pp. 2119–2132, 2002.
73. Erik Synnegård, Rolf Gustavsson, Jan-Olov Aidanpää, “Influence of cross-coupling stiffness in tilting pad journal bearings for vertical machines,” Int. J. Mech. Sci. pp. 111-112, 2016.
74. Cha M, Glavatskih S, “Non linear dynamic behavior of vertical and horizontal rotors in compliant liner tilting pad journal bearings: some design considerations,” Trib. Int. 2015; 82: 142–52. http://dx.doi.org/10.1016/j.triboint.2014.10.011. URL ⟨http://www. sciencedirect.com/science/article/pii/S0301679X14003673⟩.
75. Kang Yeong Choe, Seung Yoon On, Seung A. Song, Jun Woo Lim, Jun Il You, Seong Su Kim, “Study of the endurance performance of composite journal bearings under the oil cut situation,” Composite Structure, Vol. 134, pp. 772-781, 2015.

`

Appendix

Reynolds Equation

Reynolds provided the first analytical proof that a viscous liquid can physically separate two sliding surfaces by hydrodynamic pressure resulting in low friction and theoretically zero wear. Reynolds' theory explains the mechanism of lubrication through the generation of a viscous liquid film between the moving surfaces. The condition is that the surfaces must move, relatively to each other, with sufficient velocity to generate such a film. Lubricant pressure distribution as a function of journal speed, bearing geometry, oil clearance and lubricant viscosity is described by Reynolds equation. This equation is based on some assumptions which are as follows:

Assumptions:

- Inertia force due to acceleration of fluid, any body forces are small compared with the pressure and viscous forces terms hence, it can be neglect (i.e; $F_I = 0$, $F_B = 0$).
- Pressure variation across the film is negligibly small ($\frac{\partial P}{\partial Y} = 0$) but it varies along the length of film (P = p(x, z)).
- Curvature effects are neglected and the thickness of the film is much smaller as compared with length or width of the film.

Derivation:

By direct method- in this equilibrium of forces acting on faces of fluid elements which is dragged into a rapidly narrowing clearance space, converging in the direction of motion.

`

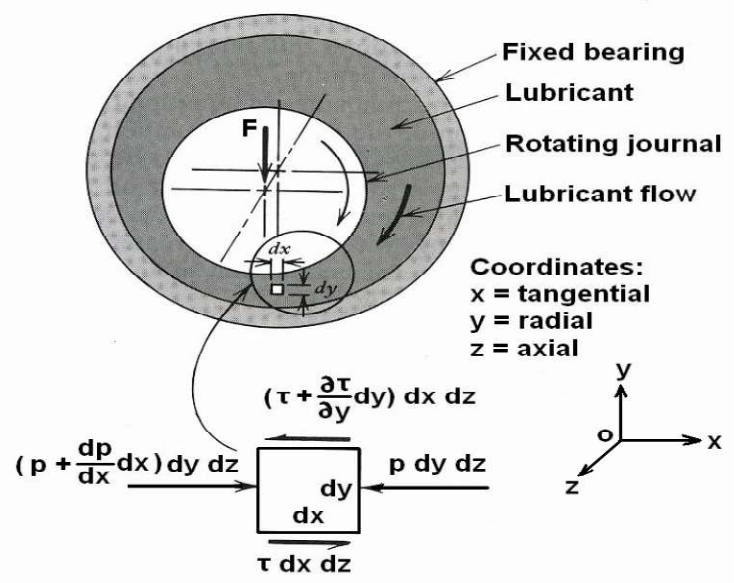

Figure 42: Equilibrium forces in X-direction.

Consider a fluid element having dimensions (dx, dy, dz) is taken in (x, y, z).

x- axis represents direction of motion of fluid.

y- axis represents radial direction of journal.

z- axis is parallel to journal axis.

<u>Velocity Distribution</u>:

- Fluid pressure force (P.dz.dy) in +x direction
- (P+$\frac{\partial P}{\partial x}$ dx) dy.dz in –x direction
- Shear force on bottom surface (τ_x dx.dz)
- Shear force on top surface (τ_x+$\frac{\partial \tau_x}{\partial y}$ dy) dx.dz

For equilibrium in x-direction-

$$Pdydz - \tau_x dxdz - \left(P + \frac{\partial P}{\partial x} dx \right) dydz + \left(\tau_x + \frac{\partial \tau_x}{\partial y} dy \right) dxdz = 0 \ldots\ldots\ldots (1)$$

`

Equation (1) reduced to,

$$\frac{\partial P}{\partial x} = \frac{\partial \tau_x}{\partial y} \text{.....(2)}$$

According to Newton's law of viscosity,

$$\tau_x = \mu \frac{\partial u}{\partial y}$$

Where, μ = dynamic viscosity or absolute viscosity of oil.(N-s/m^2)

Putting the value of τ_x in equation (2) we get,

$$\frac{\partial P}{\partial x} = \frac{\partial}{\partial y}(\mu \frac{\partial u}{\partial y})$$

Or, $$\frac{\partial P}{\partial x} = \mu \frac{\partial^2 u}{\partial y^2} \text{.....(3)}$$

Equation (3) gives pressure gradient in x-direction. Similarly pressure gradient in z & y-direction can be written as-

In z-direction, $$\frac{\partial P}{\partial z} = \mu \frac{\partial^2 w}{\partial z^2}$$

And in y-direction, $$\frac{\partial P}{\partial y} = 0 \qquad \text{(assumption (2))}$$

Where, (u,v,w) are the velocities in (x,y,z) direction respectively.

Equation (3) rewrite as,

$$\frac{\partial^2 u}{\partial y^2} = \frac{1}{\mu} \frac{\partial P}{\partial x}$$

Integrating above equation w.r.t. (y) we get,

$$\frac{\partial u}{\partial y} = \frac{1}{\mu} \frac{\partial P}{\partial x} . y + A$$

Again integrate the above equation,

$$u = \frac{1}{2\mu} \frac{\partial P}{\partial x} z^2 + Az + B \text{.....(4)}$$

`

Using boundary conditions,

At y = 0, $u = u_a = 0$ and,

At y = h, $u = u_b$

Putting these boundary condition in equation (4) we get,

$$B = 0$$

And,

$$u_b = \frac{1}{2\mu}\left(\frac{\partial P}{\partial x}.h^2\right) + A.h$$

Hence, $$A = \frac{u_b}{h} - \frac{h}{2\mu}\frac{\partial P}{\partial x}$$

By putting the value of A and B in equation (4) we get,

$$u = \frac{1}{2\mu}\left(\frac{\partial P}{\partial x}\right).y^2 + \left[\frac{u_b}{h} - \frac{h}{2\mu}\frac{\partial P}{\partial x}\right]y \text{.....(5)}$$

Rate of flow of fluid:

Rate of flow of fluid (q_x) in x-direction per unit width in z-direction is given by,

$$q_x = \int_0^h u \cdot 1 \cdot dy \text{.....(6)}$$

putting the value of 'u' from equation (5) to equation (6),

$$q_x = \int_0^h \left[\frac{1}{2\mu}\frac{\partial P}{\partial x}\left(y^2 - hy\right) + \frac{u_b}{h}y\right].dy$$

$$\Rightarrow \quad q_x = \left[\frac{1}{2\mu}\frac{\partial P}{\partial x}\left(\frac{h^3}{3} - \frac{h.h^2}{2}\right) + \frac{u_b}{h}\frac{h^2}{2}\right]$$

$$\Rightarrow \quad q_x = -\frac{h^3}{12\mu}\frac{\partial P}{\partial x} + \frac{u_b.h}{2} \text{.....(7)}$$

Similarly,we can write

`

$$q_z = -\frac{h^3}{12\mu}\frac{\partial P}{\partial z} + \frac{u_b.h}{2}$$

Continuity equation is given as,

$$\frac{\partial u}{\partial x} + \frac{\partial w}{\partial z} = 0$$

$$\Rightarrow \quad \int_0^h \frac{\partial u}{\partial x} dy + \int_0^h \frac{\partial w}{\partial z} dy = 0$$

$$\Rightarrow \quad \frac{\partial}{\partial x}\int_0^h u.dy + \frac{\partial}{\partial z}\int_0^h w.dy = 0$$

$$\Rightarrow \quad \frac{\partial}{\partial x}(q_x) + \frac{\partial}{\partial y}(q_z) = 0$$

$$\Rightarrow \quad \frac{\partial}{\partial x}\left[-\frac{\mathrm{h}^3}{12\mu}\frac{\partial P}{\partial x} + \frac{u_b.h}{2}\right] + \frac{\partial}{\partial z}\left[-\frac{h^3}{12\mu}\frac{\partial P}{\partial z} + \frac{w_b.h}{2}\right] = 0$$

$$\Rightarrow \quad \frac{\partial}{\partial x}\left[\frac{\mathrm{h}^3}{12\mu}\frac{\partial P}{\partial x}\right] + \frac{\partial}{\partial z}\left[\frac{h^3}{12\mu}\frac{\partial P}{\partial z}\right] = \frac{\partial}{\partial x}\left(\frac{u_b.h}{2}\right) + \frac{\partial}{\partial z}\left(\frac{w_b.h}{2}\right)$$

$$\Rightarrow \quad \frac{\partial}{\partial x}\left[h^3.\frac{\partial P}{\partial x}\right] + \frac{\partial}{\partial z}\left[h^3.\frac{\partial P}{\partial z}\right] = 6\mu\left[\frac{\partial}{\partial x}(u_b.h) + \frac{\partial}{\partial z}(w_b.h)\right] \text{.....(8)}$$

This equation is known as Reynolds equation in 2-D.